Ref. no. : 90-117
File no. : 8724-04350/377
Date : April 1990
NP

Title

HANDBOOK ON OBSTACLE WAKE EFFECTS RELATED TO WIND TURBINE SITING

Author(s):
J.A. Leene *
D. Delaunay **
A.G. Jensen ***

* MT-TNO P.O. Box 342
7300 AH Apeldoorn The Netherlands
** CSTB 11, rue Henri-Picherit
44300 Nantes France
*** DMI 99 Hjortekaersvej
DK-2800 Lyngby (Copenhagen) Denmark

Keyword(s):
- obstacle wakes
- wind turbine siting

Activities carried out within the framework of the CEC R & D programme on non-nuclear energy sources;
Contribution to concerted action "Wake effects";
Project "Obstacle Wake Effects"
contractnr. EN3W-0011-NL

Intended for:
Commission of the European Communities
Directorate-General for Science,
Research and Development
Rue de la Loi 200
B-1049 Brussels
Belgium

SUMMARY

On the basis of an extensive literature study a method has been developed to determine the velocity reduction in the far wake of obstacles in the atmospheric boundary layer.
Compared to the near wake this far wake is the most important with regard to wind turbine siting, as close vicinity to obstacles will mostly be avoided because of the expected hazardous turbulence effects of the approach wind on the wind loading of the wind turbine and the reduction of its power output.
An attempt is made to a systematic approach, in which all flow and obstacle effects are incorporated, although as yet not every parameter has been equally well investigated.
The method classes any obstacle shape in one of three categories: houses, trees or dikes. Main graphs give the velocity reduction for these categories, for standard conditions of the approach flow and obstacle shape. By means of correction graphs the effect of non standard conditions can be accounted for.

A validation of the method for a number of obstacle categories which shows the usefullness of the wake description method is given in an annex to this report.

Turbulence is dealt with in a limited way. The turbulence in the far wake can be estimated from graphs for the three obstacle categories, under standard conditions of approach wind and obstacle shape.
Some information about wake related features like the length of the recirculation zone close behind the obstacle and the speed-up outside the wake is given in appendices.

TABLE OF CONTENTS

Appendices: OBSTACLE EFFECTS NOT COVERED BY THE METHOD

Appendix 1 THE NEAR WAKE

Appendix 2 OBSTACLE GROUPS

Appendix 3 FLOW SPEED-UP OVER SIMPLE SHAPES

Annex: VALIDATION OF THE WAKE PREDICITION METHOD
(MT-TNO REP. 90-166)

NOTATIONS

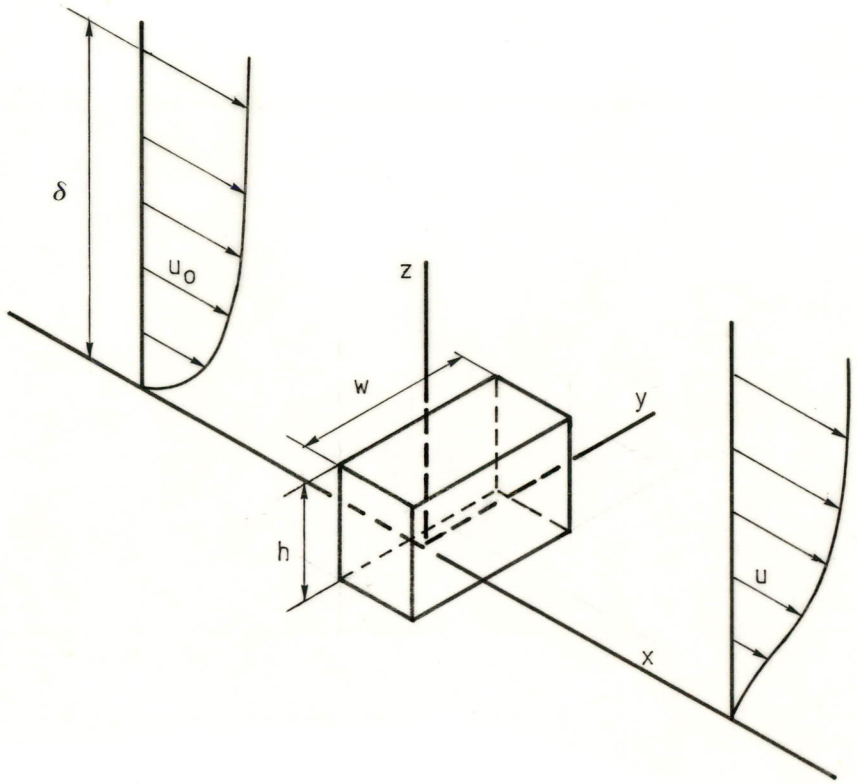

Figure 1 Notations

A_t	constant $A_t = \frac{\sigma}{u^*}$
$A(\Theta)$	wheighing function for wind direction
A	constant in near wake length expression
a	scale factor in Weibull function
a_s,n,p,E	constants in formula of Lemelin (Appendix A3)
B	constant in near wake length expression
C_B	velocity reduction factor $C_B = u(z)/u_o(z)$
D	diameter of wind turbine rotor
d	zero-plane displacement
d_o	obstacle depth
$\bar{d}$	mean obstacle depth in a group
d_h	distance between the highest point on the hill and half that value upstream in the wind direction
d_{h_o}	maximum of d_h
F_g	ground area occupied by obstacles

F_o	obstacle area normal to the wind
f(u)	Weibull distribution of wind velocities
H	height considered, hub height
h	obstacle height
$\bar{h}$	mean obstacle height in a group
h_n	height of the near wake
I	turbulence intensity $I = \frac{\sigma}{u}$
k	shape parameter in Weibull function
L	Monin-Obukhov length
L_n	near wake length
m_o	obstacle density of a group
O_g	total terrain area
P	frequency of occurrence of a wind velocity u
p	porosity
R	roughness fetch required for fully developed boundary layer
Re	Reynolds number $Re = \frac{u \cdot x}{\nu}$
Ri	Richardson number
S_o	ground area occupied by an obstacle group
ΔS	fractional speed-up factor $\Delta S = \frac{u\,(z+h) - u_o(z)}{u_o(z)}$
σ_u	standard deviation of u (turbulence)
σ_u^2	variance of turbulence
U	yearly mean wind velocity
u	flow velocity in a direction coinciding with the undisturbed wind direction, (x)
u_o	undisturbed wind velocity
w	obstacle width, lateral obstacle dimension
w_h	distance between the highest point on the hill and half that value in the across wind directions
x	down wind distance from obstacle
x_{cd}	down wind distance of constant velocity defect region
y	lateral distance
y_e	lateral distance from obstacle end
z	height
z_o	surface roughness length

α	power law exponent
β	wind direction with respect to the obstacle face (β = 0 when wind is normal)
δ	boundary layer height
δ_u	z-position of max. velocity defect
δ_t	z-position of max. turbulence defect
Θ	wind-direction with respect to North (+)
κ	von Karman constant $\kappa \simeq 0.4$
ν	kinematic viscosity
σ_u	turbulence intensity of u
$\Delta\sigma_u$	turbulence increase, see definition on page 54.
ψ	empirical stability function
φ	porosity
φ	angle between surface wind and macro wind (Coriolis effect)
λ_β	correction factor for oblique wind
λ_e	correction factor for end effect
λ_w	correction factor for finite width
λ_r	correction factor for terrain roughness
ϵ	max. velocity -or turbulence- defect in obstacle wake
γ	slope of windward obstacle face

1. INTRODUCTION

1.1 Scope

The wind power available at a site and the operational lifetime of a wind turbine can be adversely affected by nearby obstacles. For an objective judgement of the useability of a presumed wind turbine site it should be possible to determine negative obstacle effects properly in advance.
Unfortunately no general method exists to determine the flow behind an obstacle of arbitrary shape and approach wind conditions.
Only for very long so-called two-dimensional obstacles analytical descriptions have been deduced [1], but even then the correspondence with experiments is moderate.

The approach followed in this Handbook is the set-up of a graphical determination method for the flow velocity reduction and turbulence increase in the wake for real obstacles and wind conditions.
The velocity reduction is represented by

$$C_B = \frac{u(z)}{u_o(z)}$$

i.e. the velocity inside the wake with respect to the undisturbed wind velocity at the same height.
The turbulence increase is represented by

$$\Delta\sigma_u(z) = \sqrt{\text{var } u(z) - \text{var } u_o(z)}$$

i.e. the square root of the difference of the variance inside the wake and in the undisturbed flow at the same height.
The method is based on a critical evaluation of the material collected within the framework of a literature study on wakes [2].
Essentials of the method are the subdivision of obstacles in three different categories - houses, trees, dikes - because of their main specific characteristics of three-dimensionality, porosity, and two-dimensionality respectively.

For these three obstacle categories main graphs are given for the determination of the velocity reduction and the turbulence increase under standard conditions (centerline location, normal wind, smooth terrain etc.).
When conditions cannot be considered being standard, use can be made of correction graphs, allowing to use the main graphs for velocity reduction in the wake again.
With regard to the turbulence increase only main graphs and no correction graphs are given, because firstly no simple method could be obtained to account for the varying obstacle and wind flow effects, and secondly it suffices within the scope of this handbook for a judgement of the safety of the wind turbine at a specific site to use the possibly conservative data of the main graphs.

1.2 Limitations

The method describes the flow situation in the far wake, this being the most important area for wind turbine siting.
In order to be able to avoid the very strongly disturbed near wake behind a solid obstacle with its characteristic recirculating flow, the extent of this region may be estimated from the information presented in appendix 1.
For rows of trees, the near wake characterized by flow recirculation will be absent as the bleed flow through the fence prevents formation of this region.

Incidentally in a very limited area far downstream of an obstacle deviations from the flow pattern given, which is typical for a so-called momentum wake, may occur.
From some wake investigations it appears that in a small part of the wake, velocity may increase in stead of decrease due to strong obstacle-induced vortices that can transport high energy air particles from the outside into the wake region. This phenomenon may be specifically strong at oblique winds.
This favourable but very local effect is not taken into account in the Handbook method.

1.3 Users

The Handbook is first of all meant for use by wind energy application consultants and governmental authorities who are in charge of judging the useability of a possible wind turbine site.
In this respect the obstacle correction factor is just one of a number of correction factors to obtain the local wind from climatological data in a country.
A full description of all relevant parameters has been given in the recently published European Wind Atlas [3].

Except in the field of wind energy the Handbook may be used in other fields e.g. to predict cross wind effects on vehicles at highways in open country with dispersed obstacles like farms or on aircraft during take-off or landing due to flow disturbances by hangars etc.

In town planning the Handbook may be used to get an indication of the extent of the area influenced by high obstacles like appartement buildings.

Acknowledgements

- The authors greatly acknowledge the efforts of ir. P.E.J. Vermeulen of MT-TNO to interest colleagues of own and foreign research institutes, in improving the knowledge in the field of wind energy, of which the study of obstacle effects is a by-blow.

2. DESCRIPTION OF THE UNDISTURBED WIND

Before discussing the characteristics of the air flow in the lee of an obstacle a description of the undisturbed wind far upwind is necessary for different reasons.
First of all a note should be made on what is meant by "undisturbed".

Undisturbed means within the context of this Handbook, not disturbed by individual or small groups of obstacles, but a wind representative of a uniformly rough terrain to a distance of at least 50 times the obstacle height (say 1 km) from the obstacle.

- For prediction of the wind resource at a given site the undisturbed (yearly) mean local wind must be known for each wind direction sector to calculate the velocity in the wake from the C_B-graphs.
  Besides, the wake behaviour appears to be dependent to a more or less extent on the shape of the undisturbed velocity profile.
- For estimation of the fatigue loading of wind turbine or its components due to vertical wind shear both the undisturbed wind velocity and the wind profile must be known.
  Also with regard to safety, turbulence in the wake is presented in relation to the turbulence of the undisturbed wind so that the latter should be known too.

Before presenting the procedure to transform wind statistics at a meteostation to a given wind turbine site an overview is given of the wind characteristics at different scales.

2.1 Wind velocity at different scales

It is usual to distinguish wind effects at three different scales. The nomenclature used by different authors is not uniform which may be confusing.
In this handbook the nomenclature of [3] has been adopted.
The scales are macro scale, meso scale and micro scale.

- Macro scale

The macro scale is the scale at which climatological variations like depressions, sea breezes etc. take place.
The macro scale is in the order of tens of kilometers.
The macro wind velocity is defined as the mean wind velocity at great height (600 - 1200 m) above the earth surface, where the influence of surface roughness is absent.
In general the macro wind velocity is highest in coastal areas. As an illustration figure 2 presents the situation in the Netherlands [4].

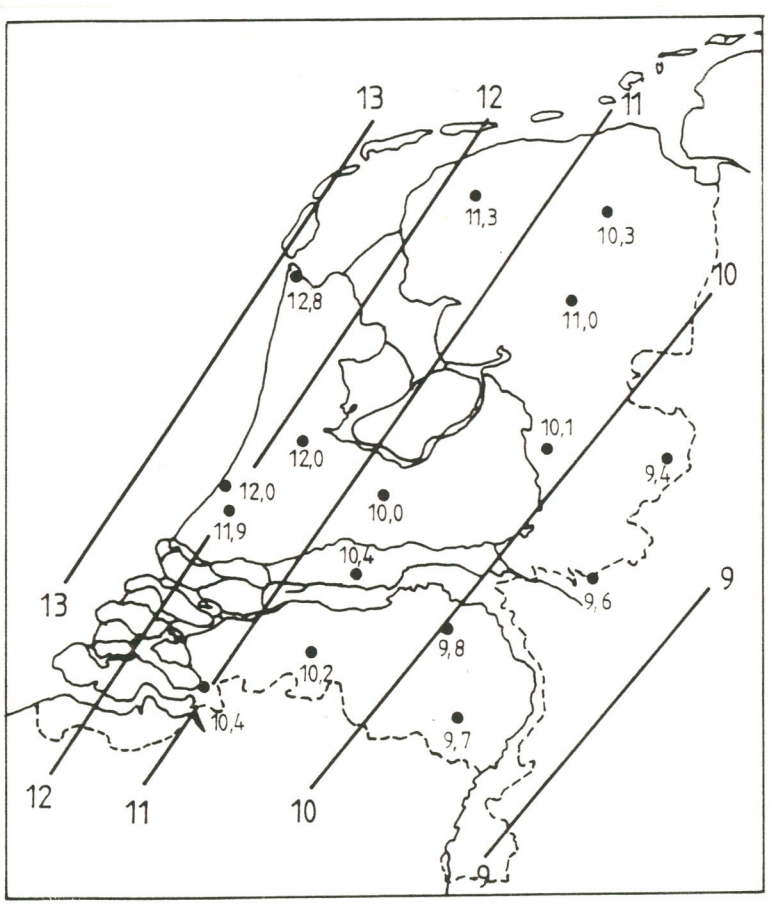

Figure 2 Example of the yearly mean macro wind velocity U_{ma} [m/s] in the Netherlands

- Meso scale

The meso scale is the scale at which the macro wind velocity is changed by regional effects, like large lakes, grass plains, woods or built up areas or combinations of these.
The meso scale is in the order of several kilometers.
As the representative regional area for Holland a square of 5 x 5 km² is taken [4].
The meso wind velocity is defined as the mean wind velocity at 60 m height.
At this height the effect of individual obstacles or local roughness is absent, and the meso wind velocity is representative for an area-averaged roughness.

- Micro scale

The micro scale is the scale at which the meso wind velocity is changed by local effects from "obstacles" like a house, tree or a dike.
The micro scale is in the order of several 100 meters to 1 km.
It is the sole subject of the Handbook.

2.2 Transformation procedure

In determining the undisturbed wind at a site from meteorological descriptions for wind stations use is made of the fact that the wind gradient in a neutral atmosphere may be described by the logarithmic law of the wall.

$$u = \frac{u_*}{\kappa} \ln \frac{z - d}{z_o} \qquad (1)$$

where u wind velocity at height z
u_* friction velocity at height z
κ von Karman constant
z_o surface roughness length
d zero plane displacement

The formula is valid down from a height d -the zero plane displacement - just below the top of the roughness elements on the earth surface up to the macro wind height.
Values for z_o and d for different terrain categories can be found in [3].

In older literature the wind gradient is often described by a power law.

$$\frac{u_1}{u_2} = \left(\frac{z_1}{z_2}\right)^{\alpha}$$

The exponent α varies from 0.1 to 0.4 dependent on terrain roughness.
A tentative relation between α and z_o is presented in figure 3.

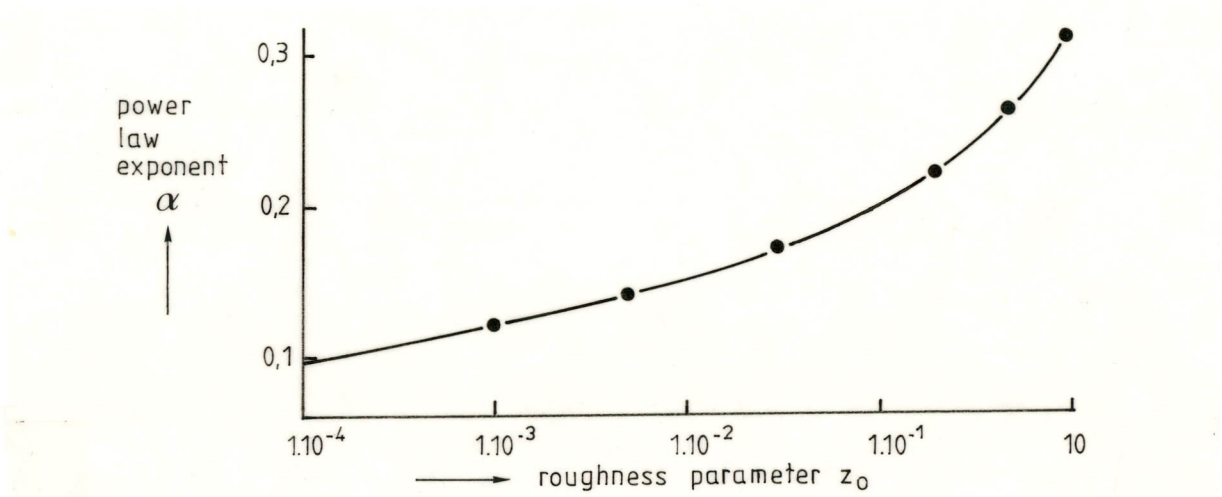

Figure 3 Tentative relation between α and z_o [5]

According to Panofsky [6] the following functional relationship exists

$$\alpha = \frac{z}{(z-d)\ \ln \frac{z-d}{z_o}}$$

with z half the height considered
d zero plane displacement

For rural terrain the formula simplifies to

$$\alpha = \frac{1}{\ln z/z_o}$$

Departing from formula 1, the undisturbed wind velocity at hub height of the wind turbine u_H can be deduced from the meso wind velocity U_{me} which in turn follows from the macro wind velocity as shown below.

In formula

$$u_H = \frac{H/z_{o_1}}{\ln 60/z_{o_1}} \cdot U_{me} \qquad (2)$$

$$U_{me} = 2.5\ U_{*_{me}}\ \ln 60/z_{o_{me}} \qquad (3)$$

$$U_{*_{me}} = 0.091\ U_{ma}\ \sin \varphi \qquad (4)$$

$$\varphi = 2.5\ \ln z_{o_{me}} - 0.23\ U_{ma} + 35.6 \qquad (5)$$

A more extensive analysis of this approach can be found in [7] from which the above mentioned deduction has been cited.

The "law of the wall" (1) on which expression (2) is based, is valid for a neutral boundary layer i.e. in general for higher wind velocities.
At lower wind velocities, of minor interest with regard to wind energy applications, the temperature built-up of the atmosphere distorts the wind gradient.
Although in the present obstacle wake prediction method of the Handbook the thermal effect cannot be accounted for, the formula for the vertical wind gradient in that case is given below for the sake of completeness.

$$u = \frac{u^*}{x} \ln \frac{z}{z_o} - \psi \left(\frac{z}{L}\right)$$

for a stable atmospheric condition $\psi = -5.2\ z/L$

for an instable atmospheric condition:

$\psi = 2\ln((1+a)/2) + \ln((1+a^2)/2) - 2\ \text{artan}\ a + \frac{\pi}{2}$

with $a = (1 - 16\ z/L)^{\frac{1}{4}}$

L is the Monin-Obukhov length which is related to the Richardson number [6].

A short description of thermal stability is presented in § 2.5.

2.3 Frequency of occurrence of wind velocity and -direction

- Wind velocity

The frequency of occurrence P of a wind velocity u, within a wind direction sector Θ can be expressed by the Weibull formula:

$$P\ [u(\Theta)] = \frac{k(\Theta)}{a(\Theta)} \left(\frac{u(\Theta)}{a(\Theta)}\right)^{k(\Theta)-1} \exp. - \left(\frac{u(\Theta)}{a(\Theta)}\right)^{k(\Theta)}$$

In this formula a(Θ) is the scaling factor which is proportional to the mean wind velocity at the meteostation and k(Θ) is the shape factor of the distribution function.

A more detailed discussion of the wind statistics is given in [3] and [5].

- Wind direction

The obstacle effect will be determined wind sector wise.
The ultimate effect on yearly power loss of a wind turbine depends on the strength of the obstacle disturbance and on the frequency of occurrence of the wind direction at which the obstacle effect is present.
Obviously not all wind directions are equally frequent.
This effect is accounted for by means of a wheighing function (figure 4).
As an example the wheighing function valid for the Netherlands is given in figure 4.

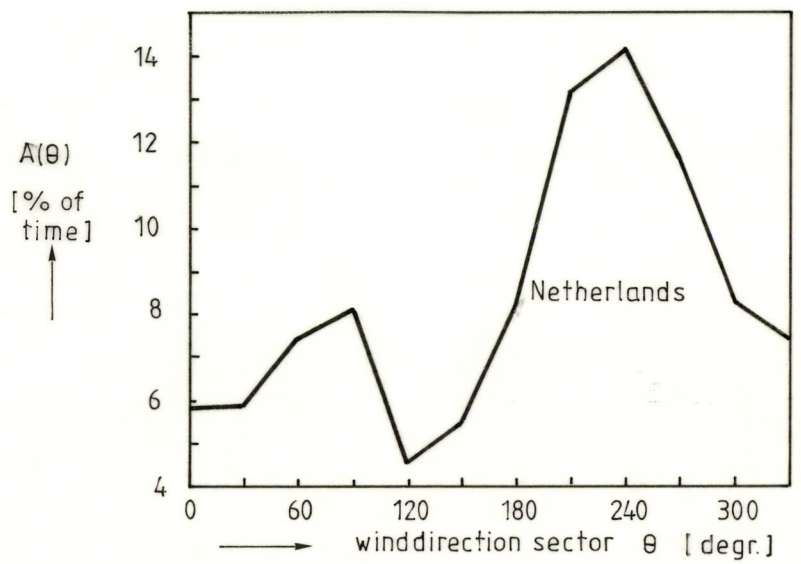

Figure 4 Wheighing functions A (Θ) for wind direction [7]

The total obstacle effect over all wind directions on the local wind velocity is given by

$$C_B = \sum_{o}^{360°} C_B(\Theta)\, A_\Theta$$

2.4 Turbulence

In purely mechanical turbulence according to Panofsky [6] a simple relation exists between the surface roughness parameter z_o and the turbulence σ_u.

$$\sigma_u = A_\tau u_*$$

In homogeneous flat terrain $A_\tau \approx 2.4$.
Substituted in (1) gives

$$I = \frac{\sigma_u}{u} = \frac{A_\tau \cdot \kappa}{\ln(z/z_o)} \qquad (\kappa \approx 0.4)$$

$$I = \frac{1}{\ln z/z_o} \quad \Rightarrow \quad \boxed{z_o = \frac{z}{e^{1/I}}}$$

2.5 Thermal stability in the atmosphere

The character of the atmospheric boundary layer is strongly determined, except by terrain roughness, by the temperature built up with height.
In the normal situation no large temperature difference exists between the ground and the air above it.
In that case the temperature decreases about 1 °C per 100 m increase in height, which is the so-called adiabatic lapse rate.
The atmospheric boundary layer is in a state of neutral stability.

A stable boundary layer situation exists when the earth surface is much cooler than the air above it. Originating turbulence will be suppressed and the wind profile will be steep.
In an unstable boundary layer situation the opposite is the case. Turbulence will be enhanced and the wind profile will be flattened (figure 5).

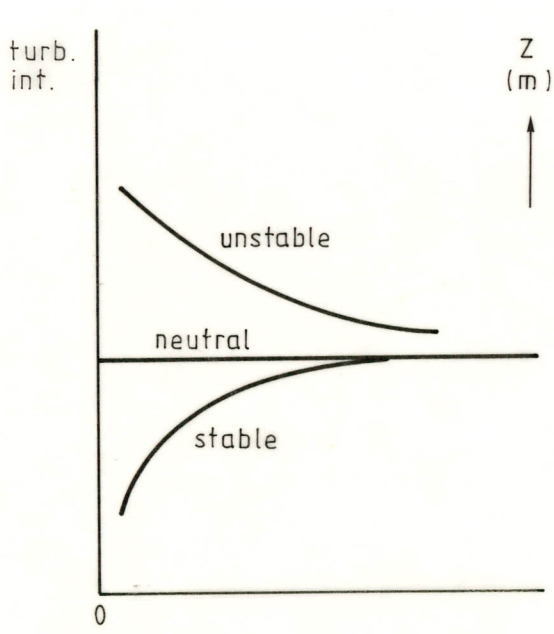

Figure 5a
Stability effect on the turbulence intensity of the wind (schematic)

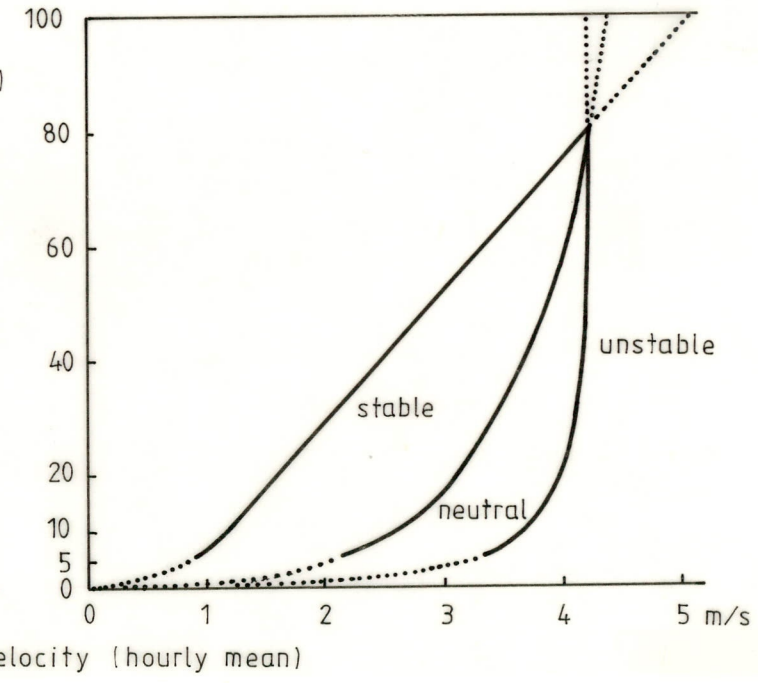

Figure 5b
Wind gradients in different conditions of atmospheric stability (schematic)

Stability effects are most pronounced at lower wind speeds (< 5 m/s) and greater heights (> 30 m).
In relatively small flat countries like Holland and Denmark neutral conditions of the atmosphere prevail by far [8-9].

Table 1 Stability classes % of time

Atmospheric situation	Holland (Schiphol) (u > 4 m/s)	Denmark (Risø) (all u)
Unstable	13	6
Neutral	78	60
Stable	9	34

As to the effect of atmospheric stability on wake development of obstacles insufficient data are available to draw conclusions.
It may be expected however that in the unstable situation the wake length will be shortened due to the increased turbulence while in the stable situation the wake length will be increased due to the decreased turbulence.
The handbook method is based on measurements of wakes in neutral boundary layers which is most often the relevant situation for wind turbine applications, where cut in speeds are normally over 4 m/s.
In some countries, with mountainous topography however the situation might be different and the use of the method may given less accurate results.
For a thorough discussion on atmospheric stability see Panofsky et al [6].

3. THE WIND DISTURBANCE BY AN OBSTACLE

A description of the way in which the local wind field may be disturbed by an obstacle can be presented in different ways.
Firstly a global description will be given, where the obstacle effect is considered as a distortion of wind field quantities without going into the character of the distortion itself.
Doing so, the effect of all relevant approach flow and obstacle parameters will be discussed, in a general sense. Secondly a more physical description of the flow as disturbed by an obstacle will be given, as it emerges from an analysis of the several studies mentioned in literature. The discussion will make clear that the actual flow phenomenae are very complex even in the case of simple situations of obstacle geometry and approach flow. However, the sensitivity of the flow development behind an obstacle to each approach flow and obstacle parameter can be demonstrated.

3.1 Global description

When seen from the passing wind flow particles the obstacle may be regarded to introduce a temporary disturbance disappearing at larger distance downwind.
The flow defect manifests itself mainly as a velocity decrease and a turbulence increase, with respect to the normal situation at that height. The maximum defect appears to remain constant up to several obstacle heights downstream.
Characteristic distances x_{cd} for a 2-dimensional and a 3-dimensional (cubic) obstacle are 10 h and 3 h respectively.
Beyond this constant defect region, the defect decays monotoneously with increasing distance.

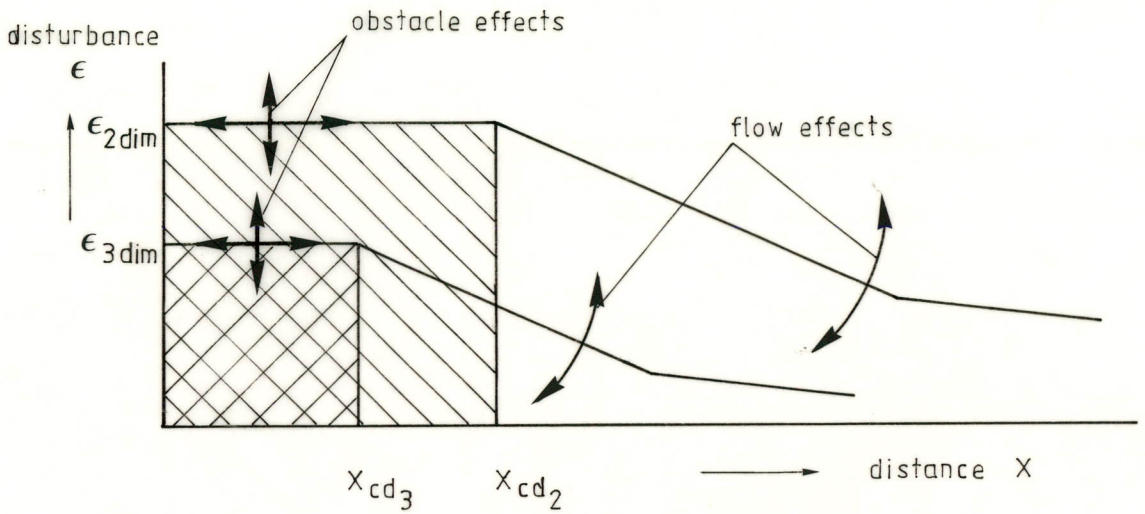

Figure 6 Wind disturbance by an obstacle

The obstacle disturbance of a wind field over homogeneous terrain as sketched in figure 6, shows much resemblance to the pulse response y of a 2nd-order system, with positive damping [10].

Some values for the turn-over points x_{cd_3} and x_{cd_2} as can be deduced from experimental results given by several investigators are presented in table 2.

Table 2 Turn-over points vel. def. lines (from Woo [11]; Mons [12])

at $h/z_o \sim 70$			at $h/z_o \to \infty$	
w/h	x_{cd}/h	x_{cd}/h	x_{cd}/h	x_{cd}/h
1	1.5	6.5	1.3	4.2
2.5	1.5	7.5	2.8	7.5
4	1.8	8.5	3.6	> 15
8.3	4.0	15.0	7.0*	
10			9	

* interpolation

From literature it appears that the maximum defect ϵ and the distance x_{cd} are mainly determined by obstacle parameters in the following descending order of significance: 1) relative width; 2) porosity p; 3) relative depth d_o; 4) obstacle geometry.

The decay of the defect, or the restoration to the undisturbed flow situation, is mainly determined by flow parameters in the following descending order of significance 5) flow direction relative to the obstacle; 6) end effect; 7) reciprocal relative terrain rougness h/z_o.

- 1) Relative obstacle width

For most man-made structures the effect of the relative obstacle width (w/h) is predominant except for very wide obstacles (w/h > 10) which will be nominally 2-dimensional.
At small w/h the maximum velocity or turbulence defect is small, while the restoration of the flow is fast by enhanced lateral mixing due to the shear layers from the side walls.
This leads to a reduction in wake length up to a factor 8, in the w/h-range from 1-10.

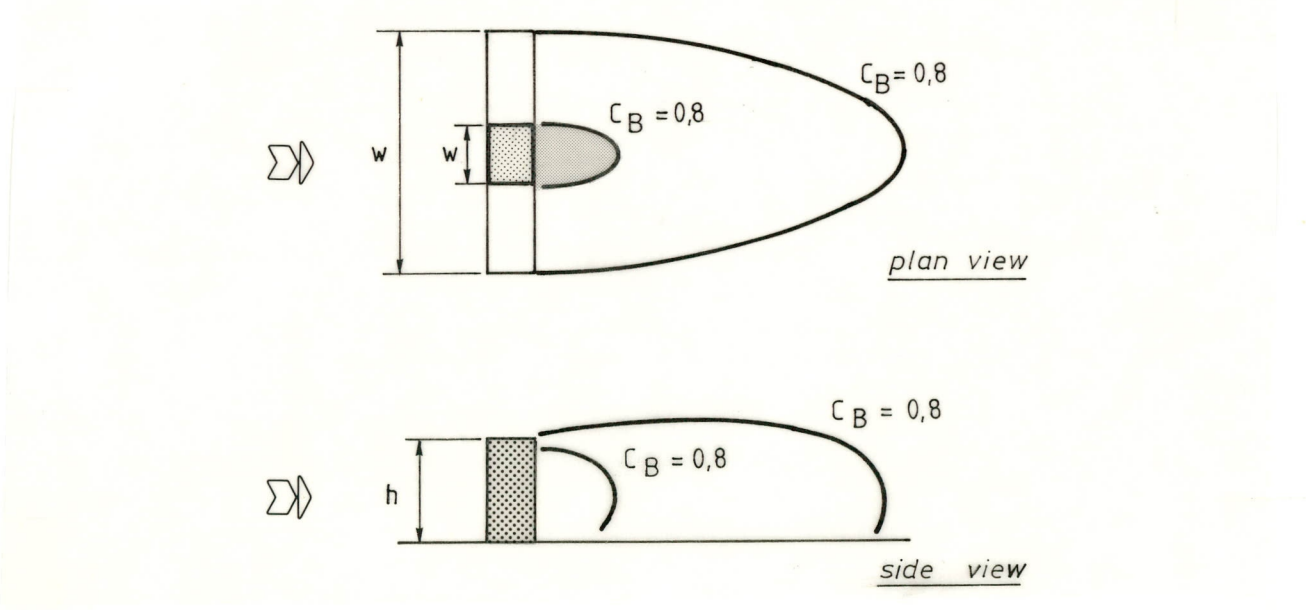

Figure 7 Effect of obstacle width on wake dimensions

- 2) Obstacle porosity p

Obstacle porosity p, is the ratio of open area to total area of the obstacle face; it mostly refers to wind screens, hedges etc.
It appears that long porous obstacles can be regarded as dense when the porosity p is less than 30%. In that case the throughflow is small, in favour of the flow over the obstacle.
At higher porosity the throughflow predominates leading to a different wake behaviour. The maximum defect of velocity as well as turbulence is less, and the wake is longer.

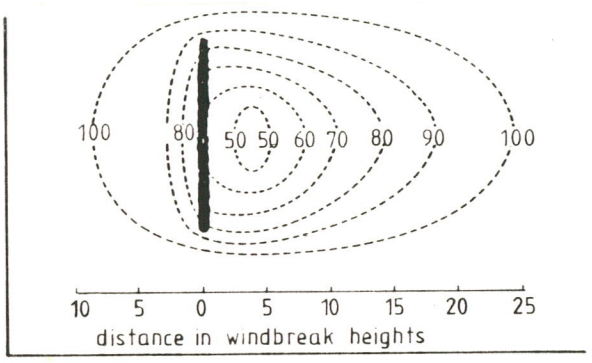

Figure 8a
Simplified diagram of reduction in wind velocity by a permeable wind break expressed as a percentage of undisturbed velocity

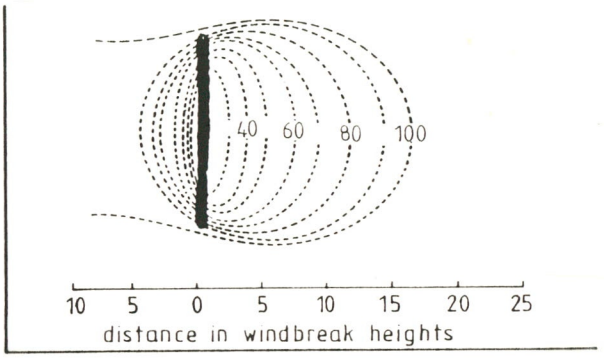

Figure 8b
Simplified diagram of reduction in wind velocity by a non- permeable wind break expresses as a percentage of undisturbed velocity

- 3) Relative depth

The effect of the relative obstacle depth d_o/h on the developing wake flow is small. Increasing depth, means an onset of streamlining by which the obstruction of the obstacle to the flow is reduced.
This results in a small decrease of the wake length.

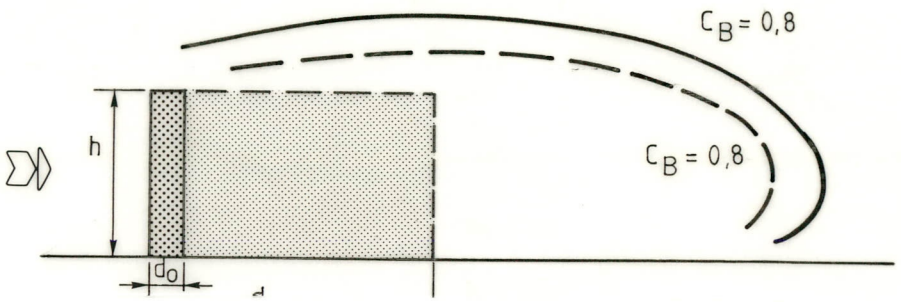

Figure 9 Effect of obstacle depth on wake dimensions

- 4) Obstacle geometry

The geometry of the obstacle plays a still smaller role.
The actual geometry may be considered as a simple block, with dimensions equal to the mean dimensions of the structure.
A faint slope of the wind face ($\gamma < 35°$) or of the lee face ($\gamma < 17°$) will result in a shorter wake.
Also for typical streamline structures, which will be rather unusual, the wake may be significantly shorter.

- 5) Flow direction

The direction of the incoming flow relative to the obstacle strongly affects the wake.
With oblique winds, the wake length will decrease especially for long (large w/h) obstacles.
It is expected that this is the effect of the constant defect region being reduced, while also the mixing of the retarded wake flow with the outer flow is enhanced.

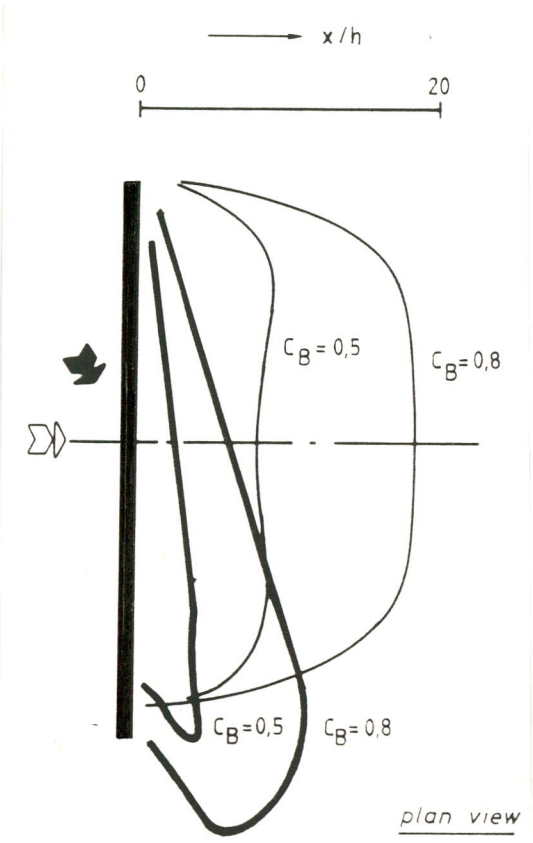

Figure 10 Effect of wind direction on the wake

- 6) End effect

At normal winds and relatively wide obstacles the length of the wake does not vary strongly, with respect to the distance from the obstacle center plane.
Close to the obstacle sides however the wake length decreases somewhat. The effect is noticeable up to 3 h from the sides inward (figure 11).

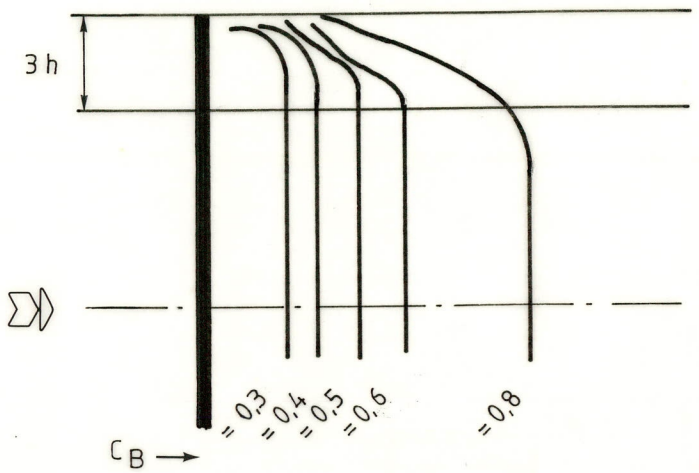

Figure 11 Obstacle end effect at normal wind

With oblique wind the end effect - especially at the upwind edge - extents to a distance much more than 3 h from the edge (figure 12).

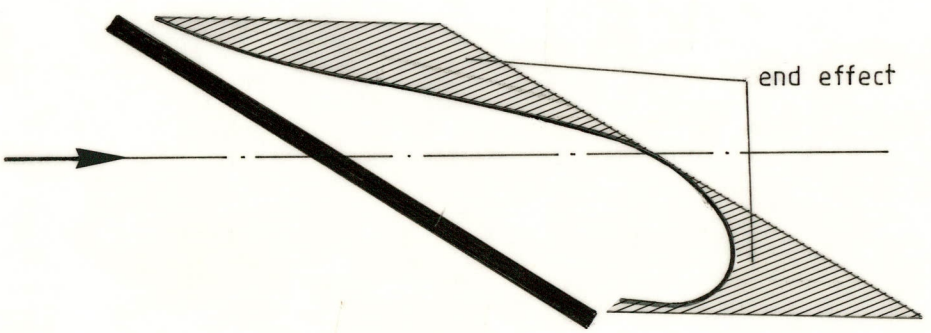

Figure 12 Sketch of area with end effect at oblique wind

This may be reason to present the correction due to end effect λ_e in dependency of the wind direction with respect to the obstacle. Lack of data, however, does not permit this approach presently and end effect is dealt with as if the wind direction is normal to the obstacle face.

- 7) Relative terrain roughness

The roughness parameter z_o characterizes the undisturbed flow over uniform terrain (see chapter 2).
At low z_o/h-value ($h/z_o > 2000$) the approach flow may be considered as smooth and uniform.

The turbulent momentum exchange at the wake boundary is low, resulting in a maximum wake length.
The effect of z_o/h is not equally strong for 2 dim. and 3 dim., and porous and solid obstacles.
At low relative obstacle width or high porosity the effect of z_o/h is small.

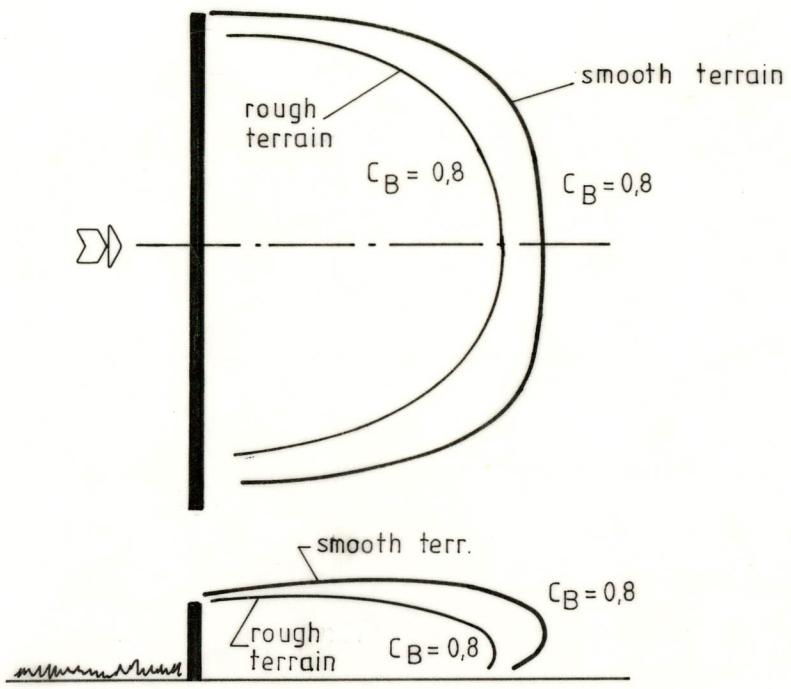

Figure 13 Effect of terrain roughness on the wake dimensions

3.2 Physical description

A description of the wake flow, or more generally the flow around an obstacle in the wind cannot be omitted in a Handbook on obstacle effects, but for the use of the method, reading of this chapter is not necessary.
The flow around an earth bound obstacle is very complex, even in the simplest case when the approach wind flow is normal to a long line-like (2 dim.) structure.
The sketches below illustrate the flows over a 2-dimensional and 3-dimensional block.

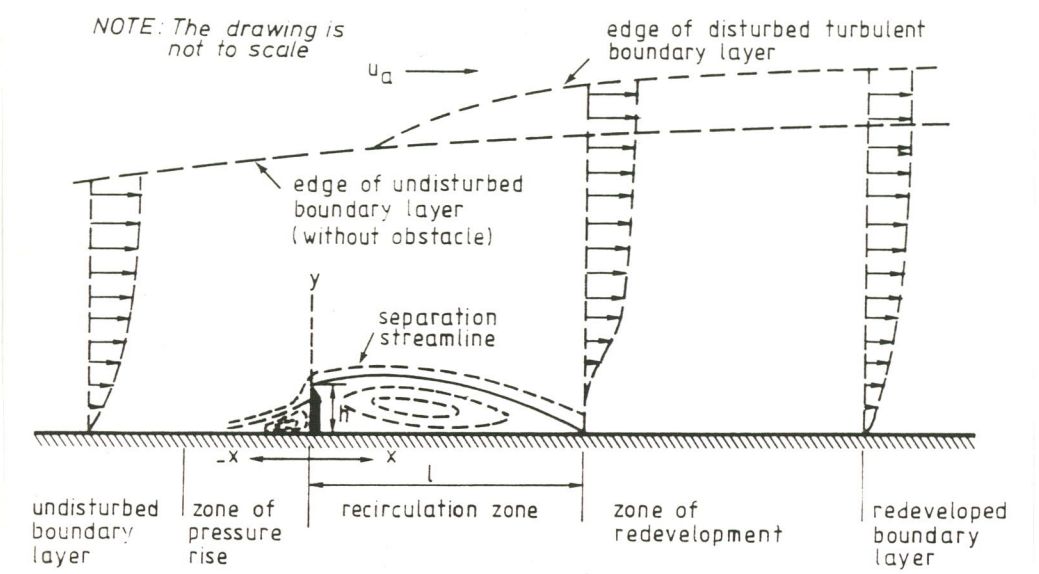

Figure 14 Flow over a 2-dimensional obstacle, from [13]

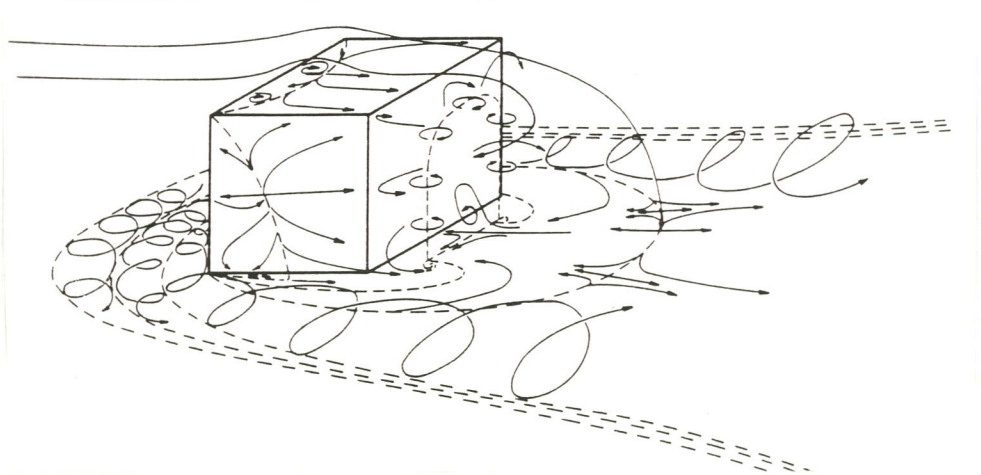

Figure 15 Flow over a 3-dimensional obstacle, from [11]

In both cases the stream lines of the approach flow, generate a standing vortex in front of the obstacle face hit by the wind.
Then the flow is deflected upward and detaches from the obstacle at the edge of the front face and the top face.
With 3 dimensional obstacles part of the approach wind can also be deflected in a lateral direction, in which case detachment also occurs at the side faces. Behind the obstacle a region develops with strong flow recirculation (except at obstacle porisities higher than 35%).

Momentum transport from the outer flow to the wake region, causes a reattachment of the flow at a certain downstream distance.
When the obstacle depth is high, reattachment may occur at the top face (roof) instead of on the ground.
From this reattachment point on, a turbulent wall boundary layer develops and sufficiently far downstream, the original velocity profile will be restored.
In the figures below velocity deficit and turbulence increase profiles are shown in the recirculation zone (x/h = 1) in the flow developing region $\left(\frac{x}{h} > 8\right)$ and in the far wake $\left(10 < \frac{x}{h} < 50\right)$.

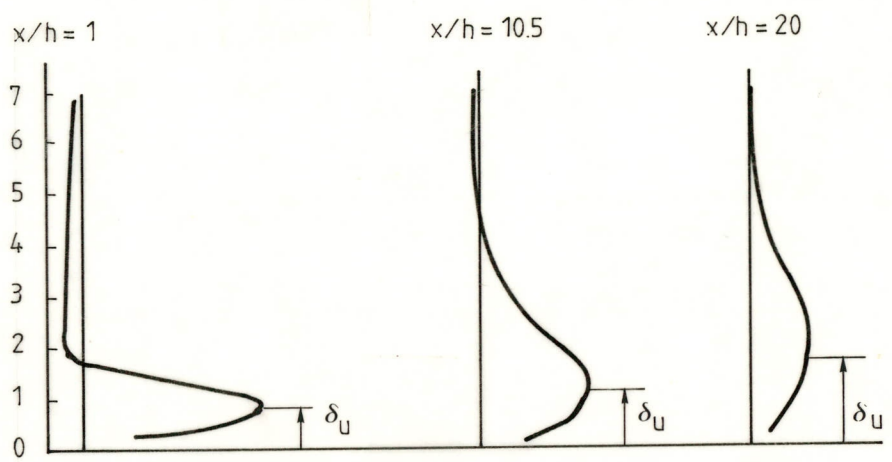

Figure 16 Velocity deficit in the wake of an obstacle, from [11]

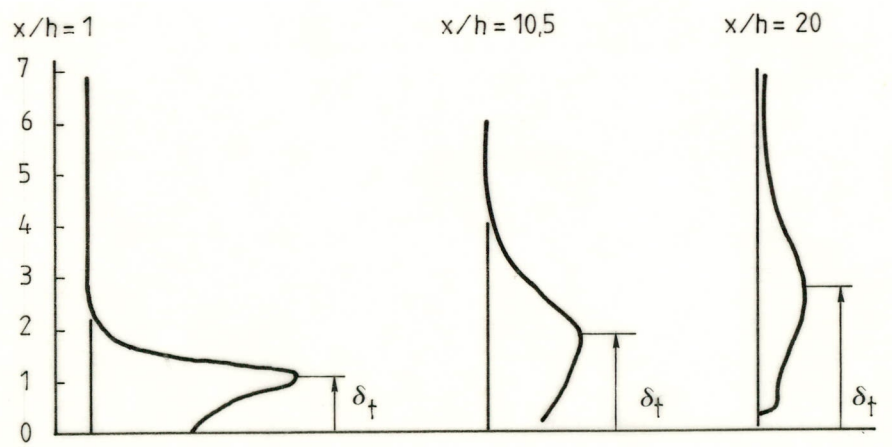

Figure 17 Turbulence excess in the wake of an obstacle, from [11]

In the far wake the velocity deficit profiles become self preserving, which means that the profiles are similar when properly scaled with h and u.

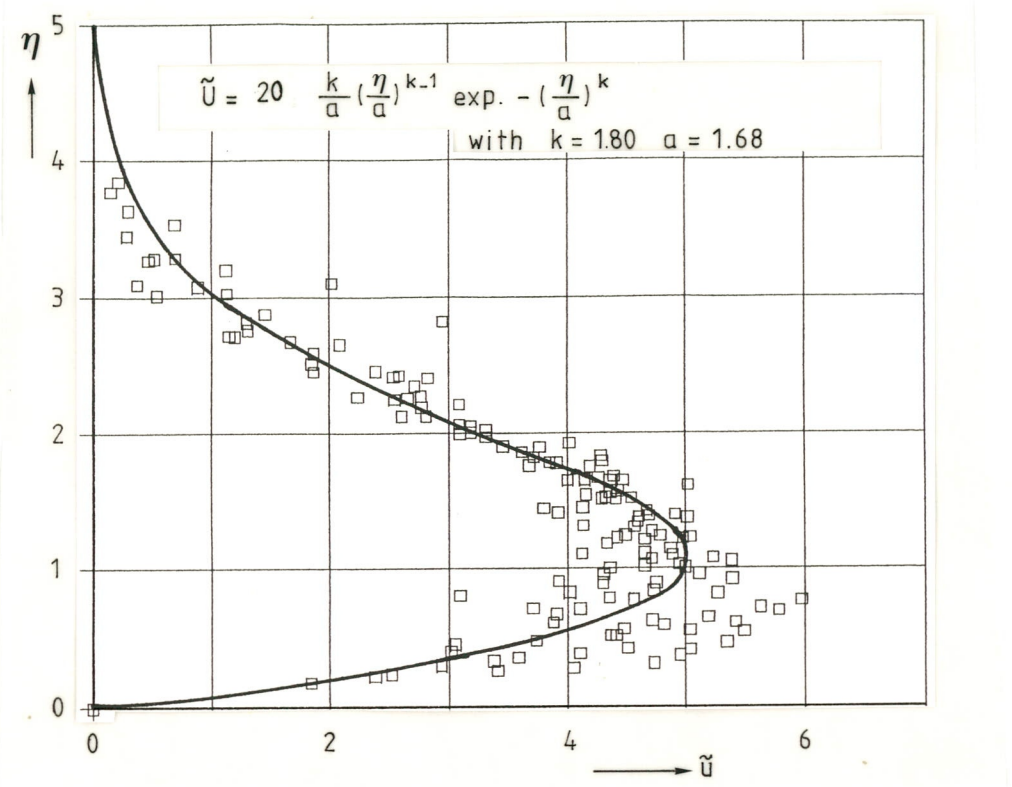

Figure 18 Velocity deficit behind a 2 dim. solid fence [14]

A reasonably good representation for the velocity deficit profile in the two dimensional case ($w/h \to \infty$) given in figure 18 is the familiar Weibull-function, which is in essence a combination of a power function (for the wall shear layer $\eta \leq 1$) and an error function (for the free outer shear layer $\eta > 1$).

$$\tilde{u} = 20 \cdot \frac{k}{a} \cdot \left(\frac{\eta}{a}\right)^{k-1} \exp - \left(\frac{\eta}{a}\right)^{k} \qquad (1)$$

with k = 1.80 and a = 1.68

$$\eta = \frac{z}{h - d} \left[\frac{\ln h/z_o}{2\kappa^2} - \frac{h - d}{x}\right]^{\frac{\ln z/z_o}{1 + 2 \ln z/z_o}} \qquad (2)$$

κ is the von Karman constant. For smooth terrain with z_o = 3 cm, d ~ o and 10 < z < 50 m formula 2 reduces to:

$$\eta = 0.59 \frac{z}{h} \left[\frac{h}{z} \cdot \ln {}^{\kappa}/_{z_o}\right]^{0.465} \qquad (3)$$

The relation of $\tilde{u}$ to fundamental flow and obstacle parameters is expressed by:

$$\tilde{u} = \frac{\Delta U(z)}{u(z)_o} \cdot \frac{\ln {}^{z}/_{z_o}}{\ln {}^{\kappa}/_{z_o}} \cdot \frac{x}{h} \qquad (4)$$

Expression 4 can also be written as:

$$\tilde{u} = (1 - C_B) \cdot \frac{x}{h} \left[1 + \frac{\ln {}^{z}/_{h}}{\ln h/z_o}\right] \qquad (5)$$

By means of 1, 3 and 5 the C_B-value can be determined for a given point P[x,y,z] in the obstacle wake.

From (2) η can be determined for a constant h/z_o-value.

Next the value of $\tilde{u}$ follows from (1). Formula (3) at last provides the C_B-value for the point P[x,y,z].

A note should be made with regard to the ${}^{h}/_{z_o}$-validity range.

The proportionality of the wake length $\left(\frac{x}{h}\right)_{max}$ with $\ln {}^{h}/_{z_o}$ as represented by expression 3 corresponds with experimental results up to an upper bound of $\frac{h}{z_o}$ which is different for 3 dimensional, 2-dimensional and 2-dimensional porous obstacles [15].
For 2-dimensional solid obstacles the upper bound will be $\left(\frac{h}{z_o}\right)_{max}$ = 2000.

In figure 18 the formula is given together with measurements from Perera, for h/z_o = 112.
The formula can be used for a first estimate of the maximal possible wake dimensions in a given situation of obstacles at a wind turbine site.

From a comparison between estimation formula and handbook curve for z_o = 0.03, z = h and h = 10 m applying the formula appears to give conservative results (see table 3 below).

Table 3 Comparison of theoretical and handbook values in the two-dimensional case

$\frac{x}{h}$	CB from formula (1) (3) (5)	CB from figure 32
13	0.51	0.70
18	0.68	0.80
33	0.86	0.90
50	0.92	0.95

The flow picture sketched so far is typically a momentum wake, which originates behind a 2-dimensional obstacle at normal wind incidence. When end-effects are taken into account or at oblique winds strong persisting "wing-tip like" vortices may originate from the obstacle (fig. 19). These vortices transport high energy air from the outer flow to the wake, so that the velocity defect may be less severe locally, or even positive.

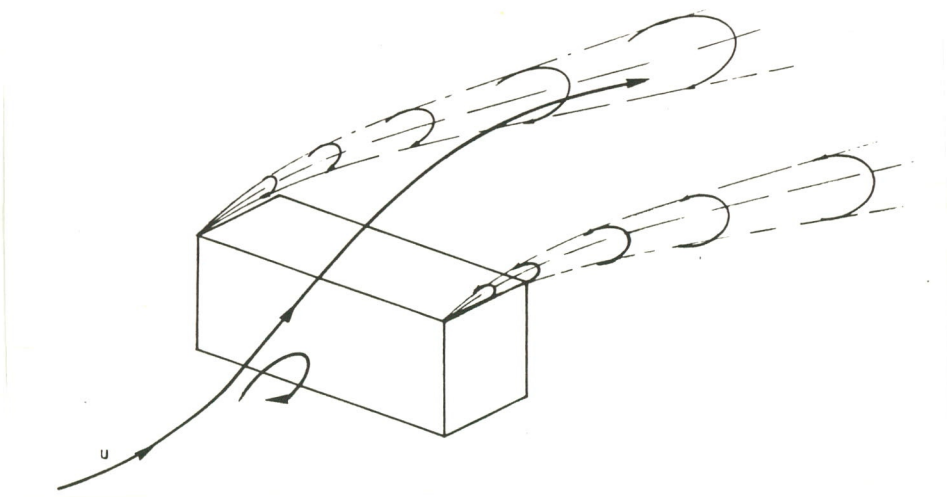

Figure 19 Sketch of momentum transport by "wing tip like" vortices

For wind energy applications it is reasonable to assume the most unfavourable flow situation - maximum velocity deficit - which is represented by the momentum wake.

A further illustration of the complexity of the flow, other than at normal situations is given for the wind direction effect and the effect of

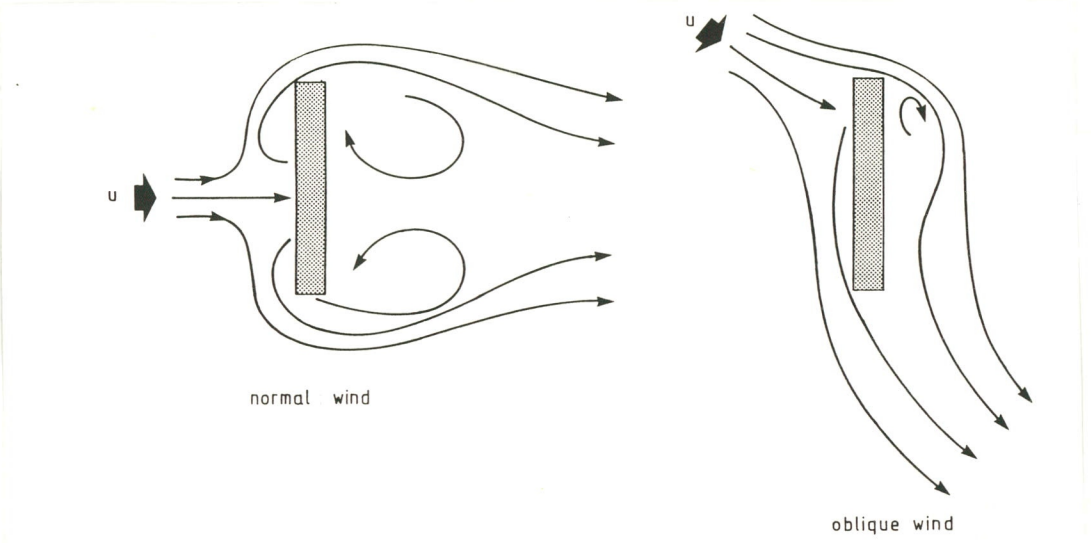

Figure 20 Effect of wind direction with respect to obstacle

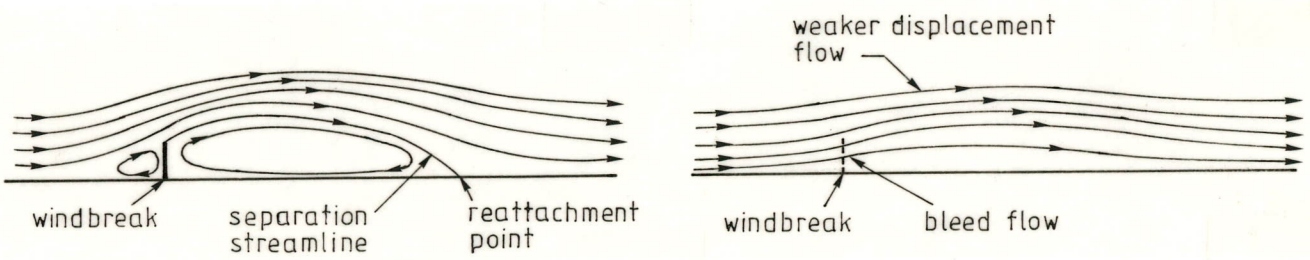

Figure 21 Streamline sketches of windbreak airflow; effect of porosity [16]

The physical effect of most other flow and obstacle parameters are not fully understood at the moment.

4. BASIS OF THE PREDICTION METHOD

4.1 Linear wake deformation

From an analysis of the results of the extensive literature study on wakes [2], it appears that to a good approximation the obstacle wake as defined by the velocity contours C_B behaves in an approximately linear way to most obstacle and flow parameters.
This means that a parameter may cause a shrinkage or an expansion of the wake, but the relative distance between the C_B-contours will remain unaltered.
Figs. 22 and 23 give an illustration of this phenomenon. The linear wake deformation concept is the basis of the method.
It makes a wake prediction method possible in which main C_B-graphs are given for well defined standard conditions and where the effect of deviating conditions can be accounted for by using correction graphs.
For the effect of the relative terrain roughness z_o/h the concept could not be verified sufficiently due to a lack of data.
However, in most practical cases when the obstacles are 3-dimensional and the relative terrain roughness is not too small ($h/z_o > 2000$) the effect is negligible.

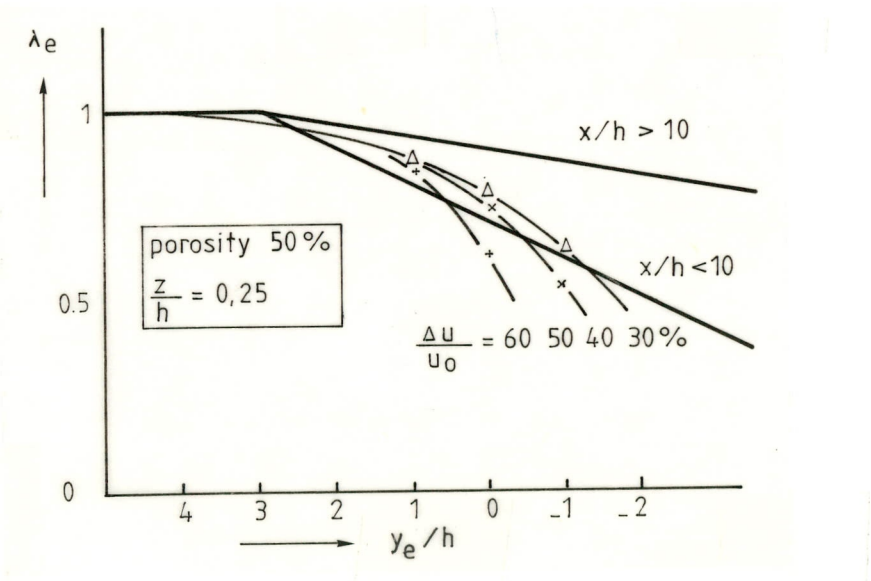

Figure 22 The effect of obstacle ends on the velocity deficit for a 50% open fence

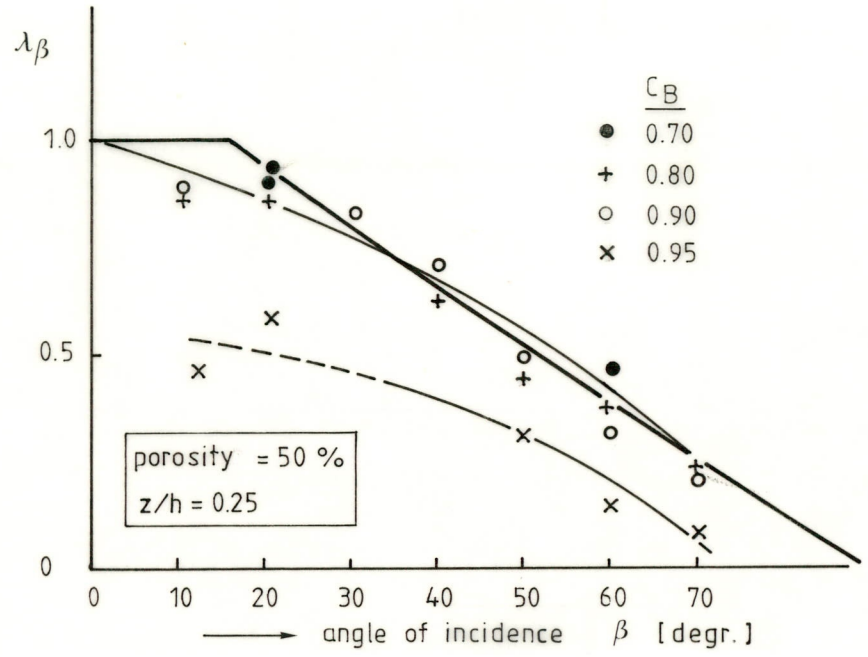

Figure 23 Effect of oblique winds

5. DETERMINATION METHOD

The first step in this determination method for wake effects of obstacles is to class a real obstacle in one of the following three categories: houses, trees, dikes.
The denominations should not be considered to strictly as they are meant as labels for structures with similar specific features, like:

- (houses) three dimensionality of the flow i.e. the wind can flow over and along the sides of the obstacle,
- (trees) the porosity allows over and through flow of the obstacle,
- (dikes) two dimensionality i.e. only flow over the obstacle is possible.

The velocity reduction and turbulence increase are given in three main graphs, to be used for standard terrain and obstacle conditions.
From correction graphs the effect of deviating conditions can be found for velocity reductions but still not for the turbulence increase.

5.1 Obstacle categorization

- Houses

Buildings, cylindrical or hemispherical gas or oil tanks, elevators, cooling towers, large ships (container, bulk, oil, etc.) in harbours and open lattice type structures.
The open structure is classed in this category, because the effect of three dimensionality normally dominates the effect of porosity.

- Trees

Hedges, artificial screens and fences.

- Dikes

In general: sudden terrain elevations or dips of over 10 h length, ridges, forward and backward facing step, elevated motorways or polder dikes. The effect of upwind or downwind slope is not considered because dikes generally have steep natural slopes (dependent on the material used) which cause flow detachment. This reduces the dike to a blunt line-like block.

An exception are sea dikes as present e.g. at several locations along the North sea coast, which may have very faint slopes. As with the backward facing step a far wake is not noticeable.

The specific geometry of an obstacle is not considered in the method, but only the main dimensions are relevant.

The geometry of the real obstacle is always schematized to a simple wall with equivalent main dimensions.
The obstacle depth need not to be taken into account.

Strictly speaking the method is valid for single obstacles only, but in some cases obstacle groups may be dealt with as well.
This depends on whether a group is to be regarded as a real group or as a general terrain roughness.
The criterion is given here and will be discussed in Appendix 2.
A real group may be substituted by a wall with the same overall dimensions, and be treated likewise as a single obstacle.

The method is restricted to the far wake of an obstacle, far away from the recirculation region.
The extent of this recirculation region can be estimated from Appendix 1

5.2 Velocity reduction factor C_B

For each obstacle category velocity reduction graphs are presented for standard conditions of obstacle and terrain.
In these main graphs $C_B = \frac{u(z)}{u_o(z)}$ i.e. the ratio of the velocity in the wake to that in the undisturbed wind at the same height, can be found for arbitrary distance $\frac{x}{h}$ from the obstacle.

The standard conditions are:
- wind direction normal
- wind plane behind the obstacle
- terrain: grass or arable land z_o = 0.03 m.

If use of the method is limited to these main graphs, a first conservative estimate of the obstacle effect is obtained.

The effect of deviations from standard conditions is given in a set of correction graphs, by means of which the actual distance from obstacle to wind turbine can be corrected to an effetive distance, x_e.

The formula reads:

$$\frac{x_e}{h} = \frac{x}{h} \cdot \frac{1}{\lambda_w \cdot \lambda_\beta \cdot \lambda_e \cdot \lambda_r}$$

where

λ_w : correction factor for finite width (fig. 33)
λ_β : correction factor for the flow direction with respect to the obstacle face (fig. 37)
λ_e : correction factor for end effects (fig. 38)
λ_r : correction factor for terrain roughness (fig. 39)

$\frac{x_e}{h}$ being determined, the actual corrected C_B-value can be found, using the main graph again.

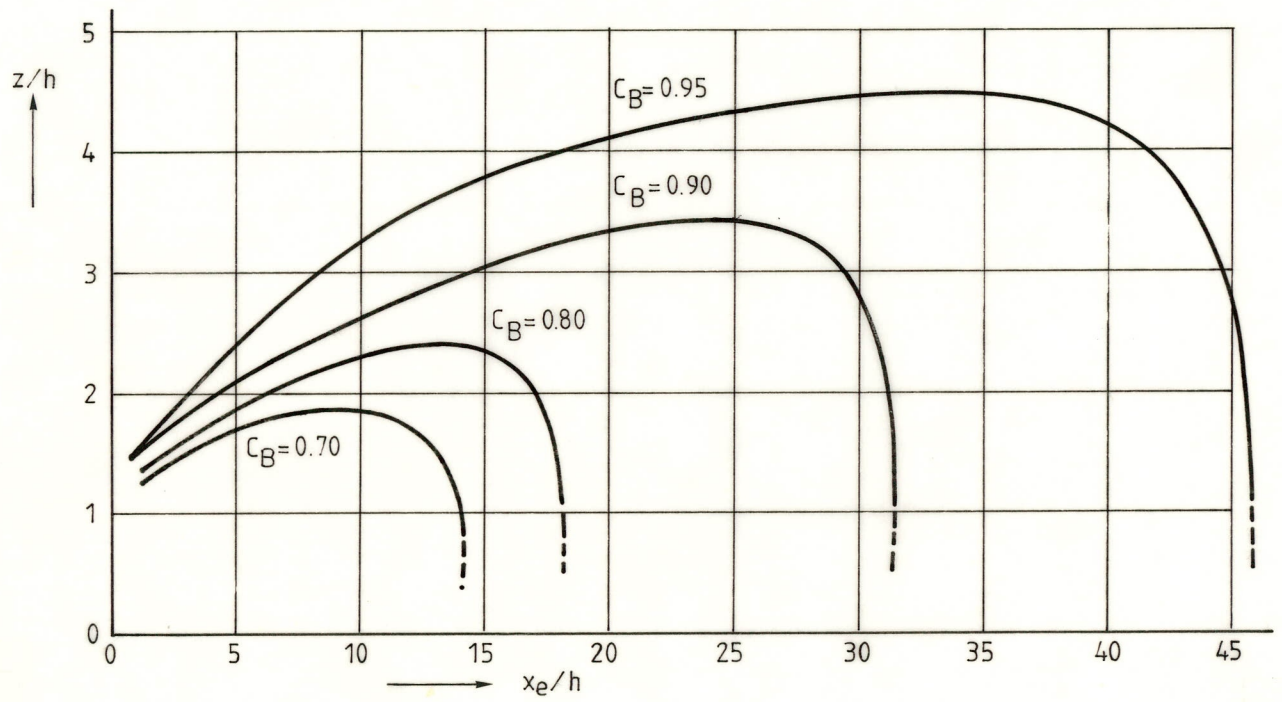

Figure 24 Main graph: Velocity ratio $C_B = u(z)/u_o(z)$ in the far wake of a house

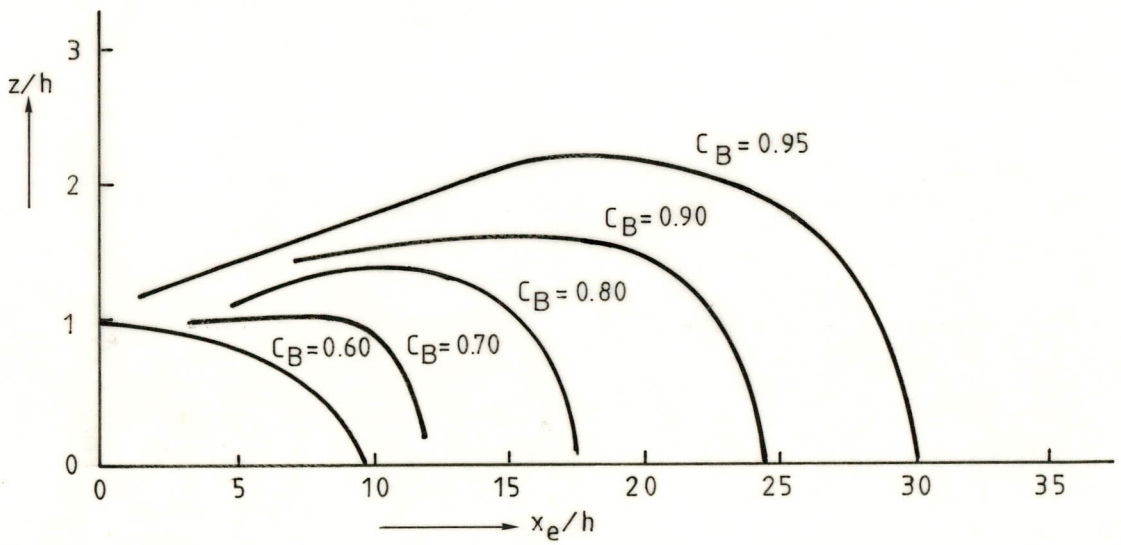

Figure 25 Main graph: Velocity ratio $C_B = u(z)/u_o(z)$ in the far wake of row of trees - porosity > 25%.

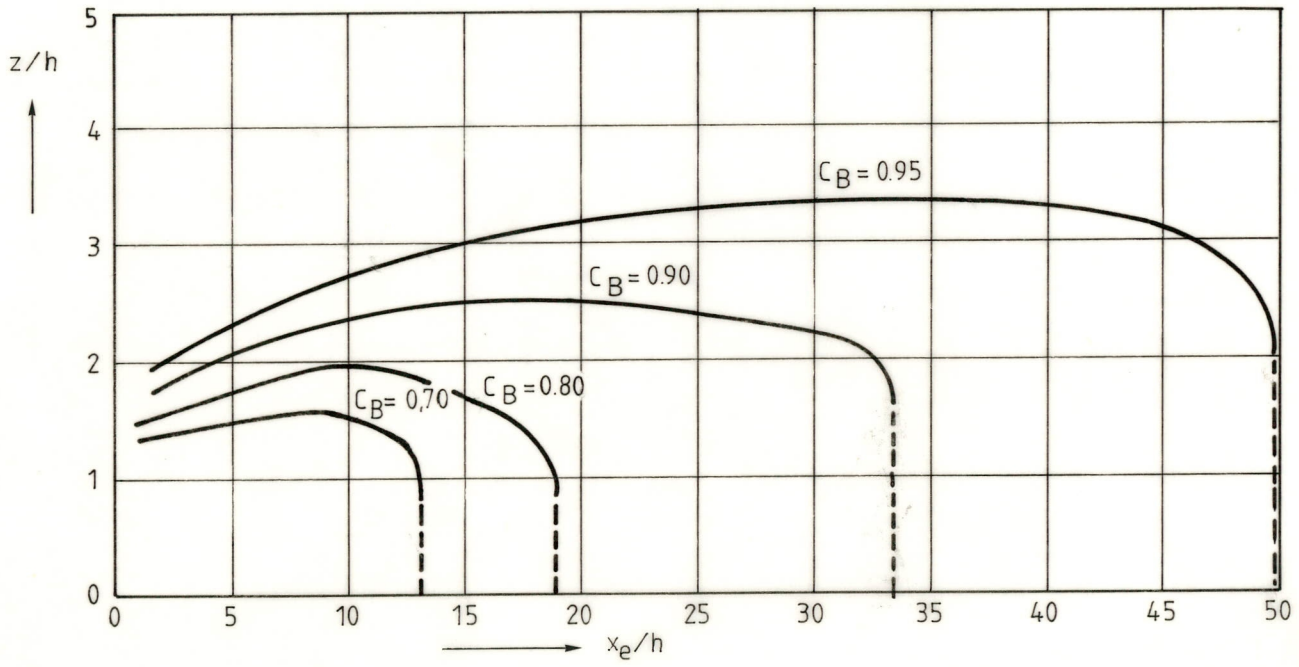

Figure 26 Main graph: Velocity ratio $C_B = u(z)/u_o(z)$ in the far wake of dikes

Next, correction graphs are given for the obstacle and flow parameters specified in 3.1

Obstacle parameters considered are width, porosity, depth and geometry.

- Width

For w/h-values smaller than 8, the effect of w/h on the dimensions of the wake is large.
At w/h = 2 e.g. the wake length x is only 30% of the wake length at w/h = 8.
The obstacle width is normally the most important obstacle parameter.

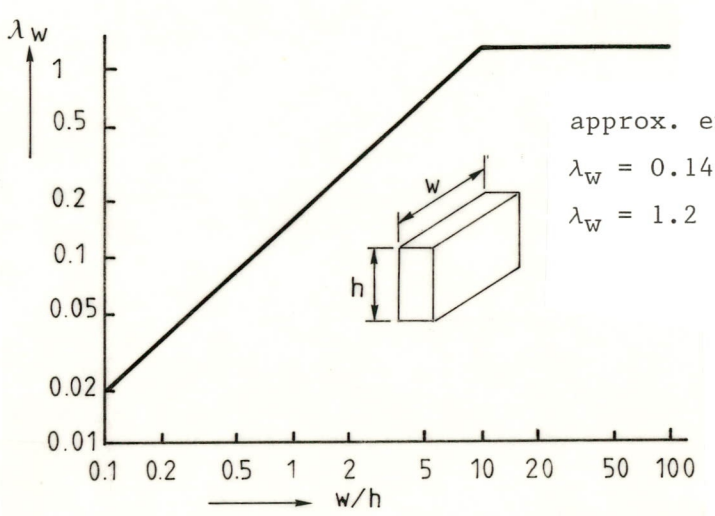

approx. expression:

$\lambda_w = 0.14\ (w/h)^{0.85}$ for $w/h \leq 10$

$\lambda_w = 1.2$ for $w/h > 10$

Figure 27 Effect of the relative obstacle width

- Porosity

No correction graph is given for porosity. Instead an overview is presented of a number of common type hedges [17] with their corresponding rank on the porosity scale.

By comparing the actual hedge type with this figure, it should be possible to estimate the porosity. For the situation in the far wake, the most important thing is to establish whether the porosity is less or over 30%.
This percentage of 30% indicates the limit between the hedge qualifications open and dense.

Figure 28 Visual determination of the porosity of natural windscreens

• Depth

A correction graph for the effect of obstacle depth is not given as this effect is only of minor importance on the far wake behaviour.
A larger obstacle depth tends to reduce the wake length slightly, and thus has a positive effect.

• Geometry

Single obstacle

The geometry of the obstacle plays no significant role in the far wake behaviour.
A specific geometry may be substituted by a wall of average height and the same width as the obstacle (see figure 29).

Figure 29 Example of plan substitute

Groups

Although the wake determination method is valid for single obstacles only it appears that obstacle groups of moderate concentration (= ratio of obstacle area normal to the wind direction (F_o) and the ground area (S_o) occupies may sometimes also be considered as a wall of equivalent height and width of the group.
This is the case if the upstream fetch of the obstacle elements is not too large.

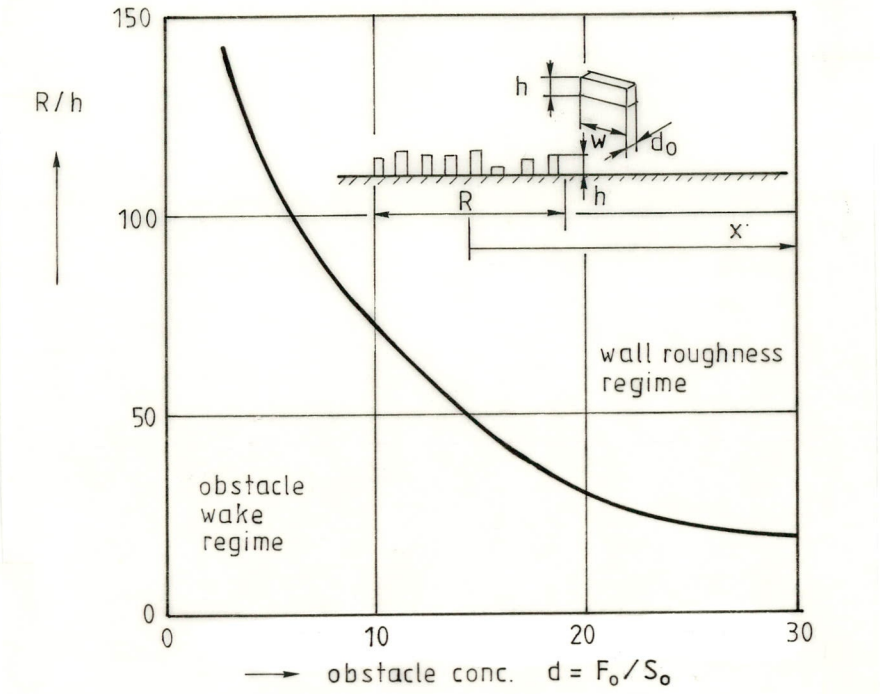

Figure 30 Fetch R required for the development of an established wall boundary layer flow (best estimate from results of [18] and [19])

By means of fig. 30 it can be determined whether a group meets this criterion.
Appendix A2 discusses the handling of obstacle groups with respect to wake determination in more detail.

Flow parameters considered are wind direction, end effect and terrain roughness.

- Wind direction

The effect of wind direction with respect to the obstacle face is strong, except in the apparent case when w/h ≤ 1 (cube, frustrum etc.) at β = 45° the wake length is almost halved.

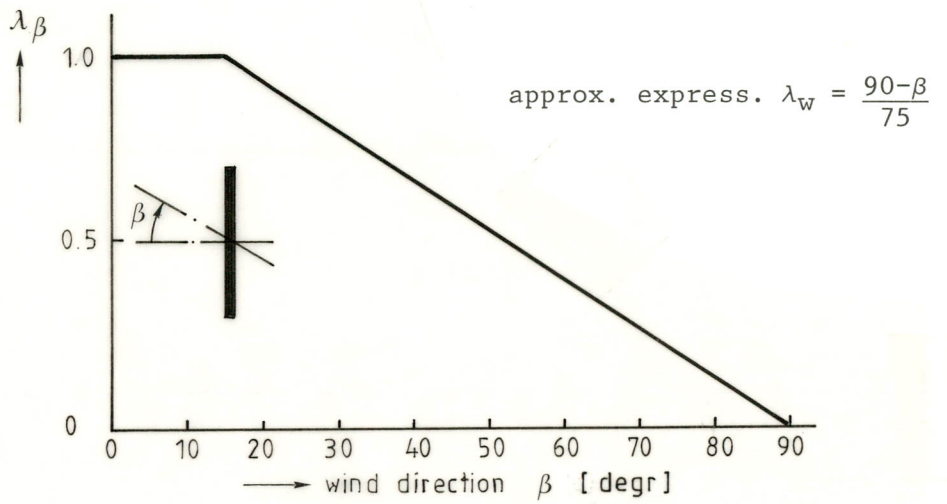

Figure 31 Effect of wind direction

- End effect

Due to the curvature of the wake near the ends of the obstacle, the length of the wake is smaller than at the center line.

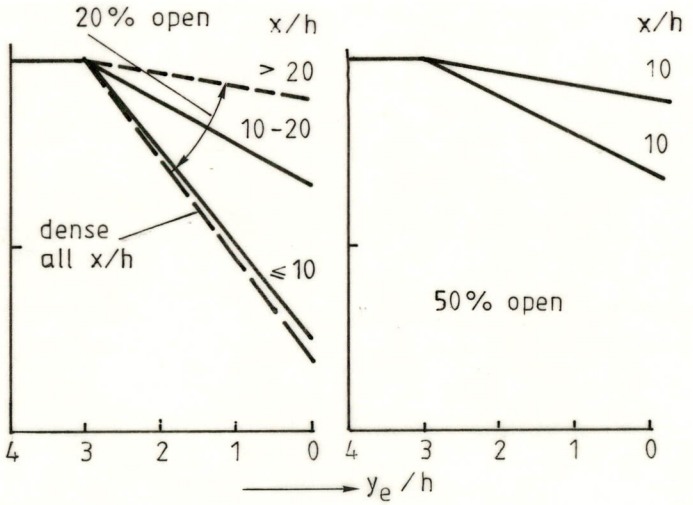

Figure 32 Obstacle end effect (y_e = 0 is obstacle end)

Fig. 32 reflects the complexity of the wake flow behind the ends of an obstacle.

The end effect is different for open and dense structures and the x/h-region. The area of influence reaches to about 3 h inward from the obstacle ends.

Terrain roughness

A high relative terrain roughness z_o in relation to the obstacle height h induces a shortening of the obstacle wake by enhanced turbulent energy transfer from the outer flow to the wake.
At large h/z_o values the effect vanishes.

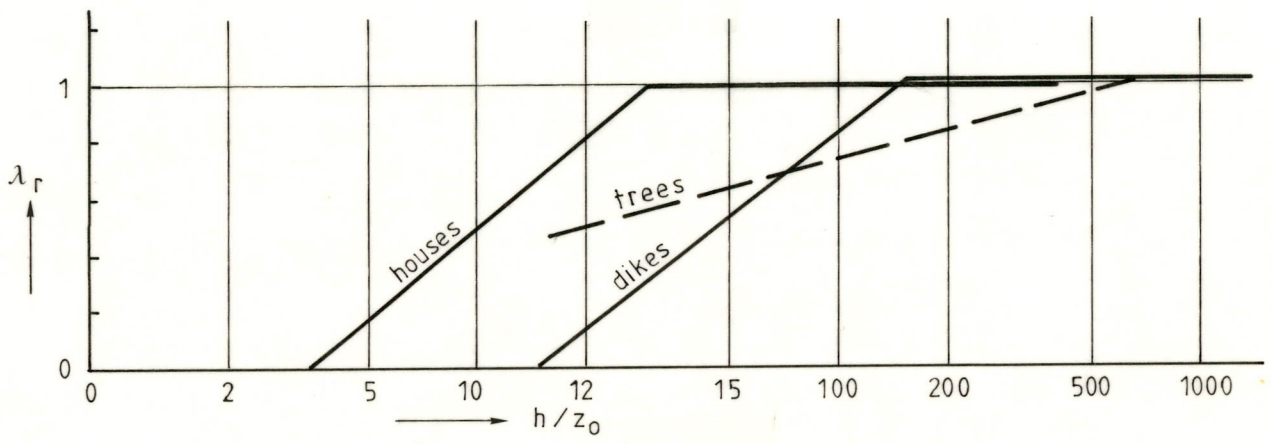

Figure 33 Effect of the relative terrain roughness z_o/h

5.3 Turbulence increase factor $\frac{\Delta \sigma_u(z)}{u(z)}$

For each obstacle category turbulence increase graphs are presented for standard conditions of obstacle and terrain only.
From these graphs an approximate value of the turbulence increase factor $\frac{\Delta\sigma_u(z)}{u(z)}$ can be found for arbitrary distance from the obstacle $\frac{x}{h}$.
The turbulence increase is defined in this handbook as the square root of the difference in variances of the velocity fluctuations in the wake and in the undisturbed flow at height z.
Thus

$$\Delta\sigma_u(z) \overset{\text{def.}}{=\!=\!=} \sqrt{\text{var } u(z) - \text{var } u(z)_o}$$

Once $\Delta\sigma_u$ at height z has been determined from the graph, the turbulence intensity $\frac{\sigma_u(z)}{u}$ can be calculated from

$$\frac{\sigma_u(z)}{u} = \frac{1}{C_B} \cdot \sqrt{\left(\frac{\Delta\sigma_u(z)^2}{u_o}\right) + \left(\frac{\sigma_o(z)^2}{u_o}\right)}$$

where $\frac{\Delta\sigma_u(z)}{u_o}$ is the graph value and $\frac{\sigma_o(z)}{u_o}$ the undisturbed value of the turbulence intensity.

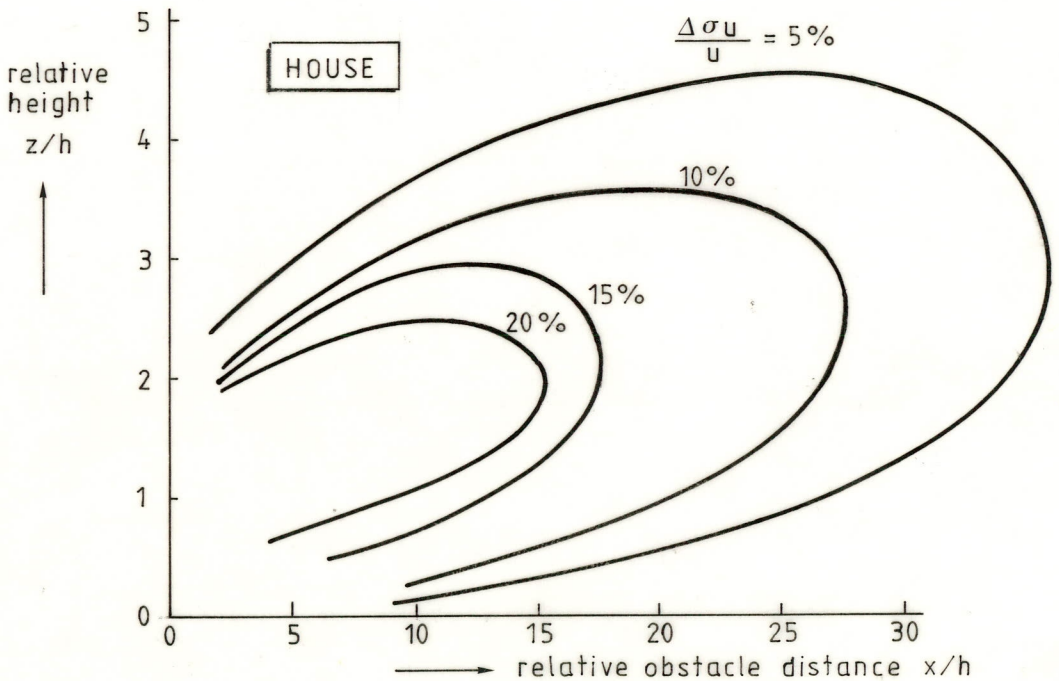

Figure 34 Turbulence increase $\frac{\Delta\sigma_u}{u}$ in the mid-plane behind a house (standard conditions)

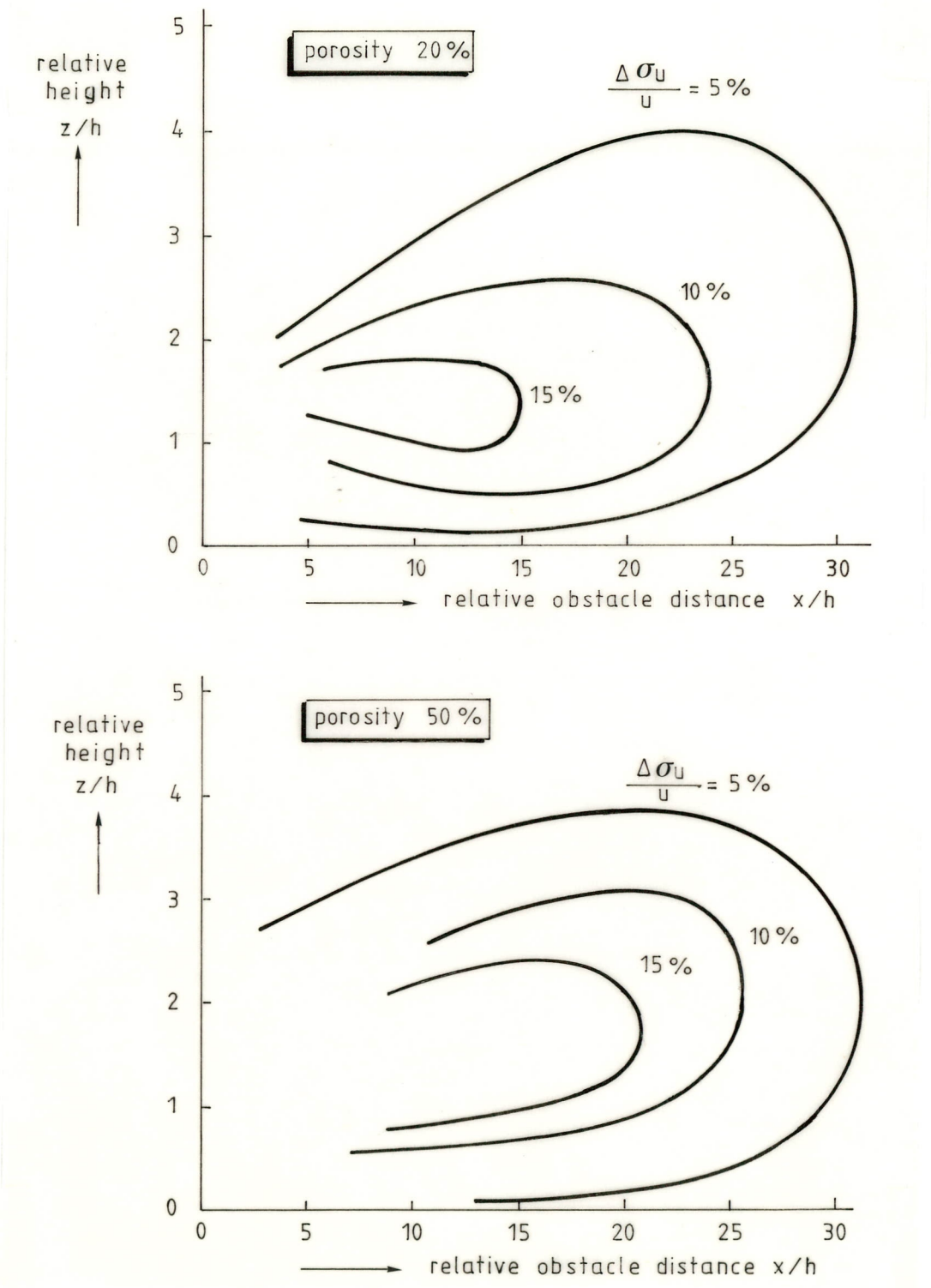

Figure 35 Turbulence increase $\frac{\Delta \sigma_u}{u}$ in the midplane behind a row of trees

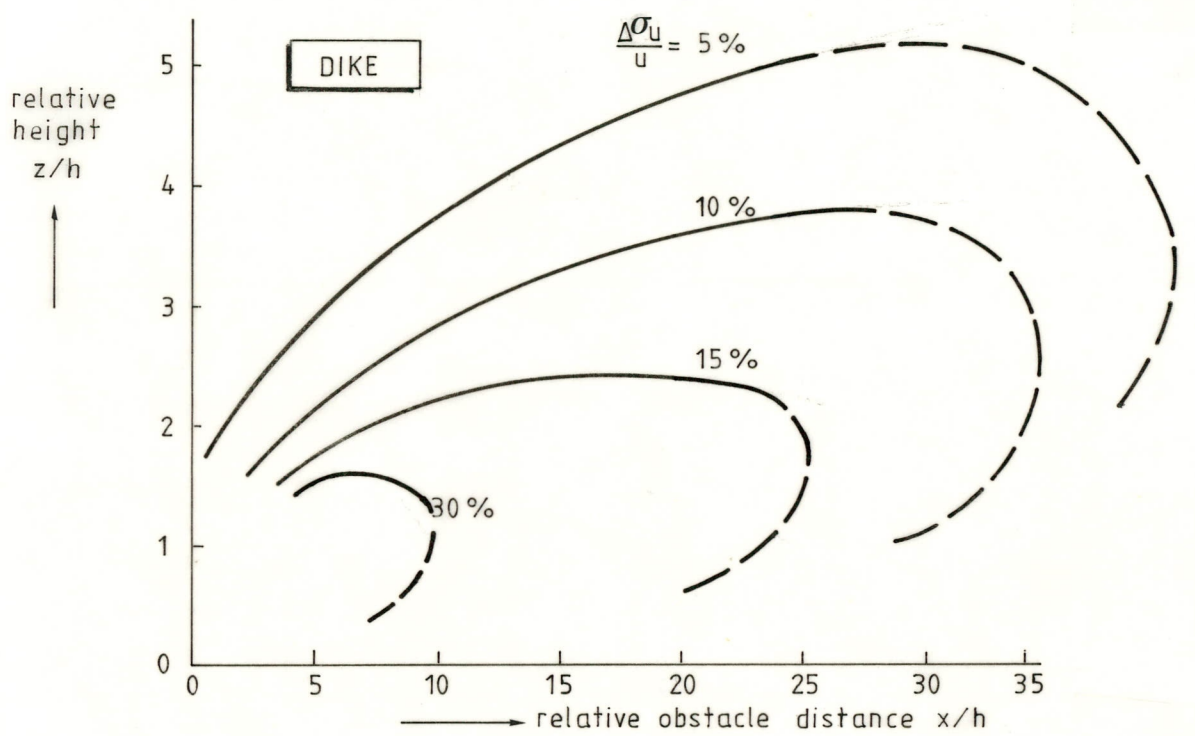

Figure 36 Turbulence increase $\frac{\Delta\sigma_u}{u}$ in the midplane behind a dike (standard conditions)

6. CALCULATION EXAMPLE

The method is illustrated by the following example of calculation of the obstacle effect.

Fig. 40 shows a fictitious example of a wind turbine site some kilometers inland from the coast. The wind turbine with a hub height of 20 m is thought to be located in the middle of the circle.

The terrain condition considered is homogeneous flat terrain with roughness length z_o = 0.03 m. (Grass or arable land)

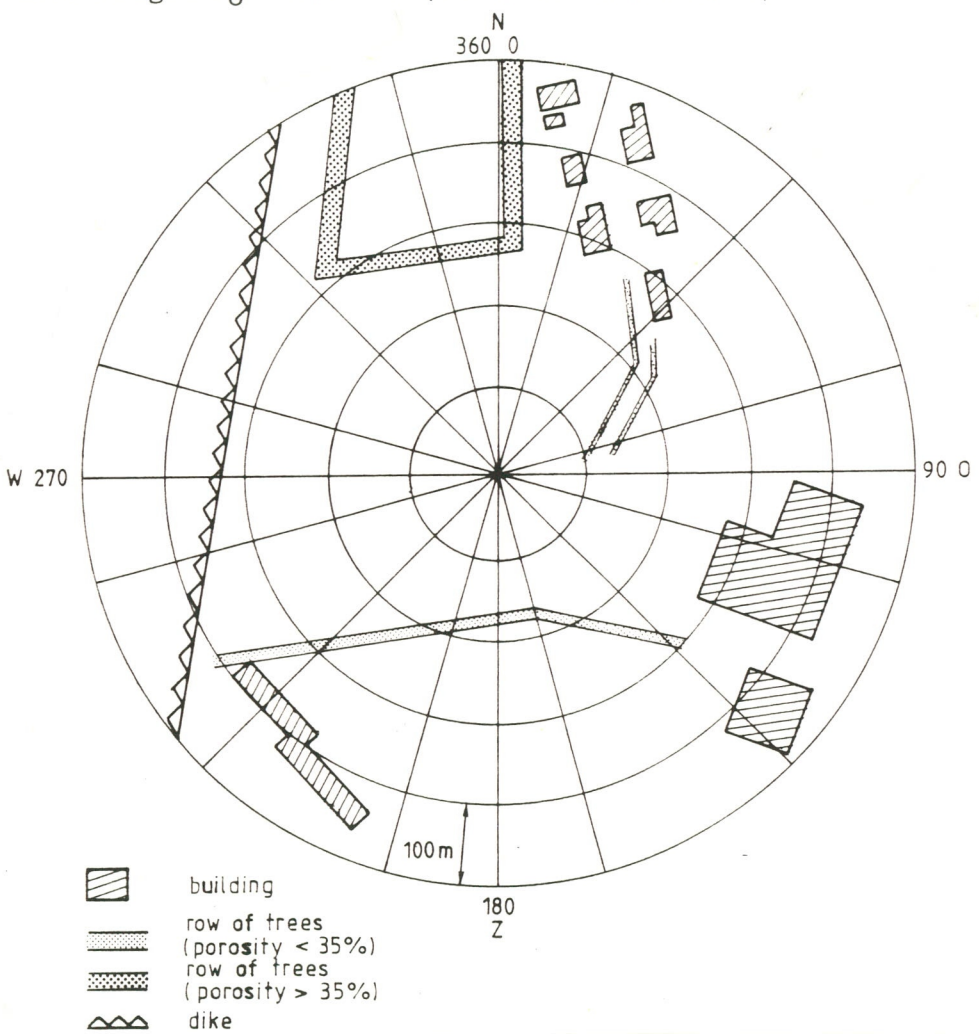

Figure 37 Wind turbine site in calculation example

The area considered is restricted to a circle with a radius of 500 m from the wind turbine.
As a rule of thumb it may be assumed that at greater distance than 50 times the obstacle height, the obstacle effect is no longer perceptible.
So the restriction of the area considered to a radius of 500 m from the wind turbine implies that at the border of this area obstacles up to 10 m height may be present.
The example is set up in such a way that all possible correction factors in determining the obstacle correction are utilized at least once.
To this end use is made of a number of different obstacles and obstacle characteristics (fig. 37).
In table 3 the successive steps in the calculation are given, resulting in the correction factor C_B.

Table 3 Calculation results of the obstacle correction factors, for the obstacles of figure 37

sector [deg]	obstacle type	x [m]	h [m]	w [m]	β [deg]	x/h	λ_β	λ_e	λ_w	λ_r	$\frac{x_e}{h}$	$\frac{z}{h}$	C_B
0	trees (<35%) (y_e/h = 2.2)												
	sector 20 deg	280	20	250	0	14	1.00	0.80	1.00	1.00	18	1.0	0.84
	houses	450	10		30	45	0.82	1.00	1.00	1.00	55	2.0	1.00
30	houses	300	10		45	30	0.65	1.00	1.00	1.00	46	2.0	1.00
60	trees (>35%)	180	9	200	30	20	0.82	1.00	1.00	0.88	28	2.2	0.91
90	shed	400	12	180	15	33	1.00	1.00	1.00	1.00	33	1.7	0.91
120	shed	400	12	180	0	33	1.00	1.00	1.00	1.00	33	1.7	0.91
	silo sector 10 deg.	450	20	100	10	23	1.00	1.00	0.70	1.00	32	1.0	0.97
150	trees (>35%)	200	9	150	45	22	0.65	1.00	1.00	0.88	39	2.2	1.00
180	trees (>35%)	180	9	350	10	20	1.00	1.00	1.00	0.88	23	2.2	0.87
210	appart. bldng												
	(sector 25 deg	400	30	200	0	13	1.00	1.00	0.60	1.00	22	0.7	0.85
	trees (>35%)	210	9	350	45	23	0.65	1.00	1.00	0.88	41	2.2	1.00
40	dike	400	5		40	80	0.60	1.00	1.00	1.00	133	4.0	1.00
	appart. bldng (y_e/h = 0.8)	400	30	200	0	13	1.00	0.40	0.60	1.00	56	0.7	1.00
	trees	350	9	300	60	39	0.40	1.00	1.00	0.88	110	2.2	1.00
270	dike	320	5		10	64	1.00	1.00	1.00	1.00	64	4.0	1.00
300	dike	350	5		20	70	1.00	1.00	1.00	1.00	70	4.0	1.00
330	trees (<35%)	300	20	250	20	15	1.00	1.00	1.00	1.00	15	1.0	0.72

In the first column the middle of the wind direction sector is given. In the second column the obstacles are mentioned.
In case of trees the porosity is also given.
Sometimes an obstacle covers only a part of the wind direction sector, which is also denoted, e.g. 20 deg. (≡ $^2/_3$ part).
Underlinement indicates that the obstacle considered is representative for the wind direction sector considered.
The following 9 colums contain input and results gained by means of the correction graphs.
The following two columns contain values from the main graphs with which finally C_B is determined, as given in the last column.

For the calculation of the obstacle correction the wind directions are subdivided in sectors of 30 deg.
These wind direction sectors are indicated in fig. 37.

The 0 deg.-sector contains wind directions between 345 deg. and 15 deg., the 30 deg.-sector between 15 deg. and 45 deg. etc.
So there are 12 wind direction sectors for which an obstacle correction factor must be determined.

- The 0 deg.-sector

In the 0 deg.-sector one finds respectively a row of 20 m high trees, of which in our example the porosity is assumed to be less than 35% and a row of houses with an average gable height of 10 m.
The distance from the row of trees to the wind turbine amounts to 280 m.
The relative distance expressed in obstacle heights becomes x/h = 14.
Successively the correction factors with which the effective distance from the wind turbine should be determined, will be calculated.

The direction of the wind relative to the obstacle is in this case almost perpendicular (β = 0°) so that λ_β = 1.0.
The width of the row of trees normal to the wind direction is 250 m, giving w/h = 12.5 which means that the row of trees may be considered as 2-dimensional.
From fig. 27 it appears that λ_w = 1.

The terrain roughness is z_o = 0.03 m for the whole area where the wind turbine is sited.
The inverse of the relative terrain roughness for this row of trees is h/z_o = 667, which leads with fig. 33 to a correction factor λ_r = 1.

The effective distance between obstacle and wind turbine is found to be

$$x_e/h = 14/(10 * 0.8 * 1.0 * 1.0) = 18.$$

The hub height of the wind turbine H = 20 m giving a relative hub height H/h = 1.

With these two parameters in fig. 25 a wind velocity reduction factor C_B = 0.76 is found.
The part of the 0 deg.-sector covered by this obstacle is 20 deg., or $^2/_3$ to C_B = 0.84.

$$C_B = {}^2/_3 \cdot 0{,}76 + {}^1/_3 = \underline{0.84}.$$

The row of houses is at a distance of about 450 m.
With an average height of 9 m this amounts to a relative distance of 50 times the obstacle height. At this distance no effect has to be expected of this obstacle according to fig. 24, C_B = 1.
Thus the largest obstacle effect is found in the 0 deg. wind sector from the row of trees (C_B = 0,84).
This wind velocity reduction factor will now be used for the whole wind direction sector.

The remaining wind direction sectors will be dealt with in the same way.
The results are presented in table 3.
The predominant reduction factor has been underlined.
It appears that in particular the appartement building in the 210 deg.-sector and the row of trees in the 0 deg., 60 deg., 180 deg. and 330 deg.-sector will have great influence.

7. REFERENCES

[1] Counihan, J. Hunt, J.C.R., Jackson, P.S.
"Wakes behind two-dimensional surface obstacles"
J.Fluid Mech., Vol 64, pp. 529-563, 1974.

[2] Leene, J.A.
"Literature study of the flow around obstacles in the natural wind"
MT-TNO rep. 83-04369 (in Dutch), 1983.

[3] Troen, I. Petersen, E.L.
"European Wind Atlas"
Risø National Lab. Denmark, 1989.

[4] Wieringa, J. Rijkoort, P.J.
"Wind climate of the Netherlands, 1983.

[5] Vermeulen, P.E.J.
"Inventarisation and evaluation of methods to determine the local wind statistics"
MT-TNO rep. 83-04376 (in Dutch), 1983.

[6] Vermeulen, P.E.J.
"A handbook for wind energy production estimates in the Netherlands" Proc. EWEC, Hamburg, 1984.

[6] Panofsky, H.A.
"Atmospheric turbulence; models and methods for engineering applications"
John Wiley & Sons, 1984.

[7] Verheij, F.J.
Handbook Energy Output of Wind turbines.
MT-TNO report 88-145, July 1989 (in Dutch).

[8] Petersen, E.L., Troen, I. et al.
"Windatlas for Denmark"
Risø National Lab. Denmark, 1981.

[9] "Climatological data of Netherlands stations,
Frequency tables of the stability of the atmosphere".
KNMI rep. 150-8, 1972 (in Dutch).

[10] Cool, J.C. et al
"Control engineering" (in Dutch)
Elsevier Amsterdam, 1977.

[11] Woo, H.C., Peterka, J.A., et al
Wind Tunnel Measurements in the Wake of Structures.
Colorado State University, June 1976.

[12] Mons, F., Sforza, P.M.
"The three dimensional wake behind an obstacle on a flat plate".
Polyd. Inst. of Brooklijn rep.nr. 68-20, 1968.

[13] Plate, E.J.
"The drag on a smooth flat plate with a fence mimersed in its turbulent boundary layer"
ASME rep.nr. 64-FE-17, 1964.

[14] Perera, S.
"Shelter behind two-dimensional solid and porous fences"
J. Wind Engineering Vol. 8, pp. 93-104, 1981.

[15] Leene, J.A.
"Obstacle wake effects and wind-turbine siting".
Delphi Wind Energy Workshop, pp.43-56, May 1985.

[16] Raine, J.K., Stevenson, D.C.
"Wind protection by model fences in a simulated atmospheric boundary layer".
Journal Ind. Aero. Vol 2, pp 159-180, 1977.

[8] Petersen, E.L., Troen, I. et al.
"Windatlas for Denmark"
Risø National Lab. Denmark, 1981.

[9] "Climatological data of Netherlands stations,
Frequency tables of the stability of the atmosphere".
KNMI rep. 150-8, 1972 (in Dutch).

[10] Cool, J.C. et al
"Control engineering" (in Dutch)
Elsevier Amsterdam, 1977.

[11] Woo, H.C., Peterka, J.A., et al
Wind Tunnel Measurements in the Wake of Structures.
Colorado State University, June 1976.

[12] Mons, F., Sforza, P.M.
"The three dimensional wake behind an obstacle on a flat plate".
Polyd. Inst. of Brooklijn rep.nr. 68-20, 1968.

[13] Plate, E.J.
"The drag on a smooth flat plate with a fence mimersed in its turbulent boundary layer"
ASME rep.nr. 64-FE-17, 1964.

[14] Perera, S.
"Shelter behind two-dimensional solid and porous fences"
J. Wind Engineering Vol. 8, pp. 93-104, 1981.

[15] Leene, J.A.
"Obstacle wake effects and wind-turbine siting".
Delphi Wind Energy Workshop, pp.43-56, May 1985.

[16] Raine, J.K., Stevenson, D.C.
"Wind protection by model fences in a simulated atmospheric boundary layer".
Journal Ind. Aero. Vol 2, pp 159-180, 1977.

[17] Sturrock
"Aerodynamic studies of shelter belts in New-Zealand"
N.Z.J.Sci. 12/15, 1969/1972.

[18] Hussain, M.
"A study of the windforces on low rise buildings and their application to natural ventilation design methods"
Univ. of Sheffield, 1978.

[19] Vermeulen, P.E.J.
"Inventarisation and evaluation of methods to determine the local wind statistics".
MT-TNO rep. 83-04376, 1983.

Reports published as part of the Handbook project (exc. progress reports).

[20] Leene, J.A.
"Review of Previous Studies on Wake Effects of Obstacles in relation to Wind Turbine Siting at MT-TNO. MT-TNO rep.87-145, May 1987.

[21] Calvez, H. et Couchman, C.
"Measures in situ des effects d'une haie sur le vent" (with English Summary). CSTB rep. EN-CLI 87.6 L, June 1987.

[22] Delaunay, D. and Duchêne-Marullaz.
"Evaluation of previous relevant work carried out by CSTB on wake structure of trees and hedges". CSTB note, June 1987.

[23] Ingham, P.
"Evaluation of Previous Wind tunnel Studies at DMI concerning the Influence of Buildings on the Energy Production of Wind Turbines". DMI Techn. Note SL 87835, September 1987.

[24] Bisgaard, C. and Ingham,
E.E.C.-Project: "Siting of Wind Turbines near Buildings and Obstacles"; Status for DMI Wind-Tunnel Investigations. DMI Techn. Note DMI 87835, October 1987.

[25] Delaunay, D.
"Full Scale Experiment of Wake Structure behind a Hedge".
CSTB rep. EN-CLI 88.11. R, June 1988.

[26] Leene, J.A., Delaunay, D., Jensen, A.G.
"European Handbook on Building and Obstacle Effects on Wind Turbine Siting". Proc. Int. Wind Energy Conference Herning, Denmark, June 1988.

[27] Jensen, A.G.
"Siting of Wind Turbines near Buildings and Obstacles".
DMI rep. 87835, September 1988.

8. AUTHENTICATION

- Name and address of the principal:

  Commission of the European Communities
  Directorate-General for Science,
  Research and Development
  Rue de la Loi 200
  B-1049 Brussels
  Belgium

- Names and functions of the co-operators:

  J.A. Leene
  D. Delaunay
  A.G. Jensen

- Names of establishments to which part of the research was put out to contract:

  Centre Scientifique et Technique du Batiment
  11, rue Henri-Picherit
  44300 Nantes France

  Danish Maritime Institute
  99 Hjortekaersvej
  DK-2800 Lyngby (Copenhagen) Denmark

- Date upon which, or period in which, the research took place:

  1-07-1986 to 30-09-1989

- Signature:

ir. L. van de Snoek
research coordinator

Approved by:

Ir. B. Stork
Head of the Department

Appendices:

OBSTACLE EFFECTS NOT COVERED BY THE METHOD

Appendix 1 THE NEAR WAKE

Appendix 2 OBSTACLE GROUPS

Appendix 3 FLOW SPEED-UP OVER SIMPLE SHAPES

Appendix 1 THE NEAR WAKE

The flow region downstream of an obstacle placed in the wind can be divided into the near wake and the far wake.
While the flow disturbances in the short near wake are maximal, they decrease gradually in the much longer far wake.
The flow in the near wake is beyond the scope of this handbook but with regard to the choice of a wind turbine site the extent of this region is of importance.

Locating wind turbines in this near wake region is dissuaded, not merely because of the smaller amount of wind energy available but especially because of the strong dynamic wind loading of wind turbines due to high turbulence intensities and wind shear.

- Flow characterization

The flow region immediately behind an obstacle in the wind, is of such a complex nature that only a global description can be given.
It is that part of the wake where the wind field perturbance is maximal in terms of velocity decrease and turbulence increase, while the static pressure is minimal.
The region is also characterized by a strong recirculating flow. The perturbed near wake flow is a result of the phenomenon that the incoming wind flow cannot follow the sudden transitions of the obstacles front face into the roof and side faces. Instead, the flow detaches from the obstacle surface and remains so for some obstacle heights downwind.
If a certain x/h is exceeded, the flow reattaches to the ground and from then on a more regular wake evolves.

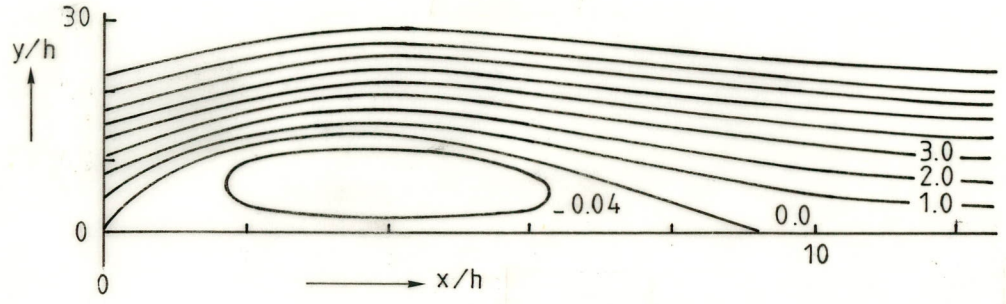

Figure 1.1 Flow field in the separated and reattached regions, Re = 2.80 x 10^4

The strongly disturbed flow region is indicated by investigators as:

- recirculation region
- wake cavity
- wake bubble/separation bubble
- reversed flow region
- separated region
- "dead water" region

Within the context of this handbook the term near wake will be adopted. The near wake is defined (criterion a) as the flow region downwind of an obstacle, where the flow velocity decrease and the turbulence increase is (almost) constant with respect to the approach wind flow (see chap. 3, fig. 6).
This is in contrast with the far wake behaviour, where the flow perturbations decrease with increasing distance from the obstacle.
Unfortunately the amount of data available to determine the near wake length thus defined is limited to a small range of obstacle and flow parameters while the variability of wake lengths is large [1, 2].
Therefore use is made of wake lengths which have been measured according to other criteria like:

b. - Location where the flow at ground level is no longer in reverse direction (by means of tufts).

c. - Location of zero static pressure gradient

$\frac{\Delta p}{\Delta x} = 0$ (or $p = p_{max}$)

d. - Location where there is no longer zero skin friction (normal for separated flow).

Although these different ways of near wake determination do not give exactly the same result as Ota [3] has shown for method b. to d., the correspondence is good enough for establishing the x/h value where the near wake ends and the far wake for which the determination method has been evolved begins.

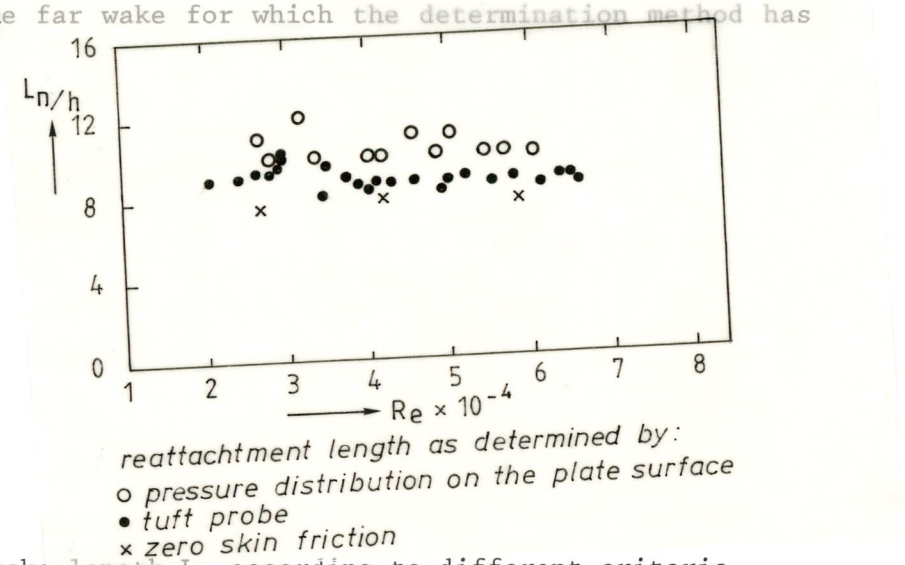

Figure 1.2 The near wake length L_n according to different criteria

- Dimensions of the near wake

As the boundary of the near wake is curved (see sketch below) the near wake length will be a function of height. Up to $\frac{z}{h} = 1$ the wake length is unique with respect to $\frac{z}{h}$ but when $1 < \frac{z}{h} < \frac{h_n}{h}$ the wake length is double valued.

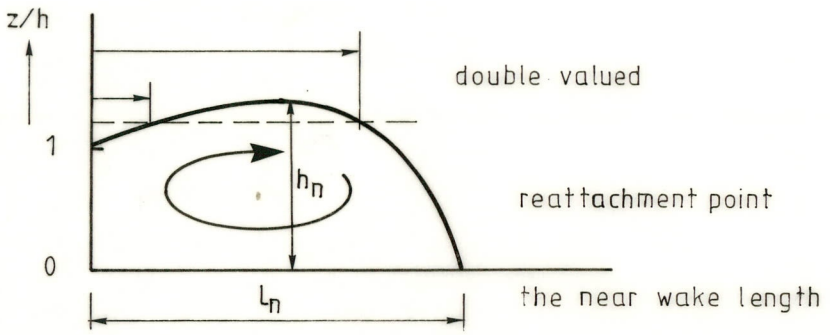

Figure 1.3 Definition of near-wake length

Like in literature only the length of the recirculation zone at ground level $(\frac{z}{h} = 0)$ will be regarded here.

The same obstacle- and flow parameters that determine the shape of the far wake play a role in the formation of the near wake. A difference is that obstacle "details" like the depth to height ratio are important.

The effect of a large relative depth of an obstacle is, that the flow after being detached at the front face to roof transition will reattach to the obstacle surface at a point (line) some obstacle height down wind.

Normally, reattachment of the flow will take place beyond $\frac{x}{h} = 2$ from the obstacle leading edge, but in very smooth flow reattachment will be delayed.

From the work of Fackrell [4] who defines the recirculation length L_n as the point downstream of the obstacle where the static pressure gradient $\frac{\Delta p}{\Delta x} = 0$ it appears that L_n may be expressed by

$$L_n = 1.8\ w/h\ [(d_o/h)^{0.3}(1 + 0.24\ w/h)]^{-1} \qquad (1)$$

The variability of L_n in the range of width to height $0.5 < w/h < \infty$ and (inverse) relative roughness $60 < h/z_o < 1800$ appeared to be less then ± 10%.

It is suggested to use $d_o/h = 0.3$ if $d_o/h < 0.3$ and $d_o/h = 3$ if $d_o/h > 3$ but no validation beyond these extremes has been made.

Instead of formule 1 a simpler expression may be used which covers Fackrells experimental results in the w/h-range tested, while the predicted wake length for w/h → ∞ agrees fairly well with values given in literature for two-dimensional obstacles in an atmospheric boundery layer. This formula reads

$$\frac{L_n}{h} = 6.3 \left(\frac{d_o}{h}\right)^{-0.3} \quad [1-\exp -0.2\ w/h]$$

For the within the context of the handbook less relevant situation of very smooth approach flow and w/h > 5 the formula of Hosker [5] gives a better representation of the measuring results.

$$L_n = \frac{A \cdot w/h}{1 + B.w/h}$$

with A = 1.75 and B = 0.25 for $d_o/h > 2$

and $A = 2 + 3.7\ (d_o/h)^{-1/3}$; $B = 0.15 + 0.3\ (d_o/h)^{-1/3}$ for $d_o/h < 2$.

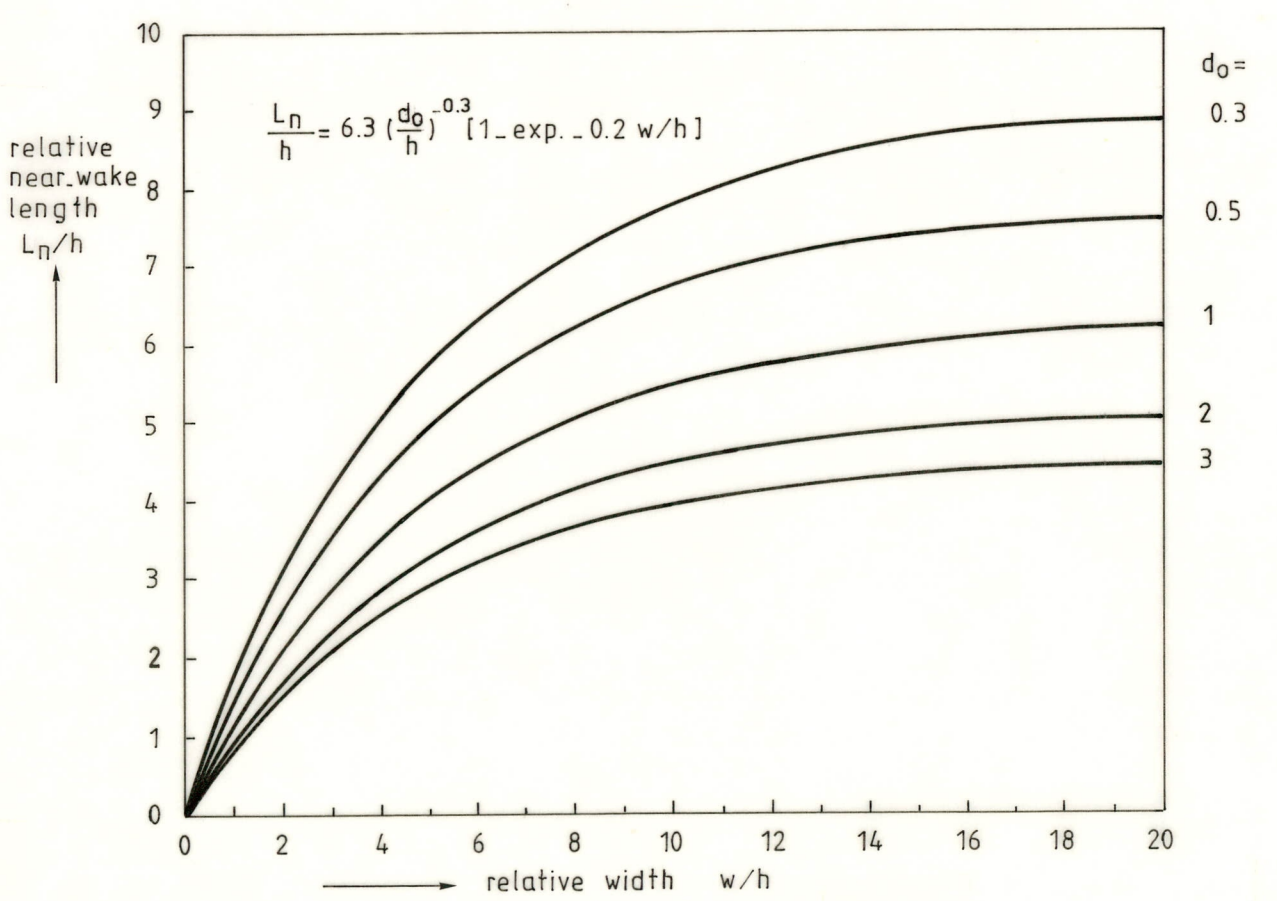

References

[1] Woo, H.G.C.
"Wind tunnel measurements in the wakes of structures"
Colorado State Univ., 1976.

[2] Logan, E.
"Wind tunnel measurements of the three dimensional wakes of buildings"
NASA, rep. 3565, 1982.

[3] Ota, T., Itasaka, M.
"A separated and reattached flow on a blunt flat plate".
J. Fluids Engineering, pp. 79-86, March 1976.

[4] Fackrell, J.E.
Parameters characterising dispersion in the near wake of buildings.
Journ. Wind Energy, Vol. 16, pp. 97-118, 1984.

[5] Hosker, R.P.
Empirical estimation of wake cavity size behind block type structures.
Turb. Diffusion and Air Pollution, Symp., Reno, Nevada, Jan. 1979.

Appendix 2 OBSTACLE GROUP

2.1 Obstacle concentration

The effect of an obstacle group on the local wind velocity field cannot be simply deduced from the method developed for isolated obstacles.
In order to be able to establish the approach that should be followed when obstacle groups are present the concept of obstacle concentration is introduced. This obstacle concentration is defined as the ratio of obstacle area normal to the direction of the wind (F_o) and the ground area (F_g) occupied. The following subdivision will be made.

A. Low obstacle concentration ($F_o/F_g < 0.01$)

In a situation of very scattered obstacles the flows about each individual obstacle do not interfere.
The situation is comparable with that of isolated obstacles, for which the given method is valid.

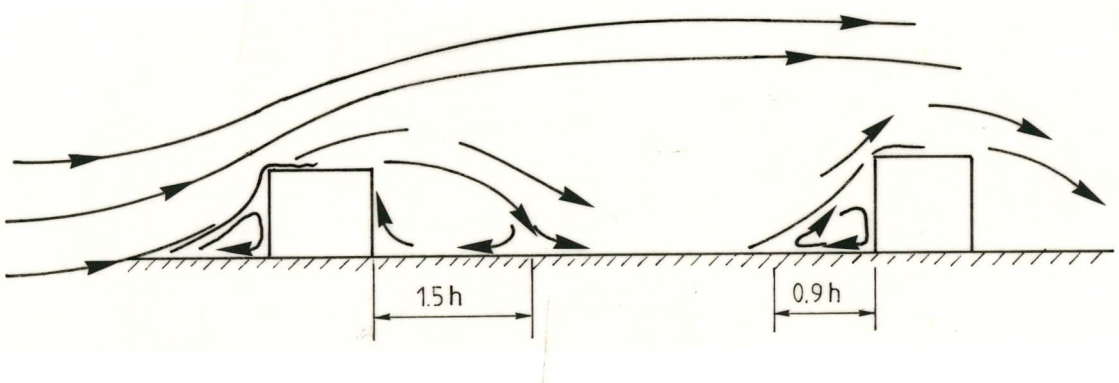

Figure 2.1 Low obstacle concentration-schematized flow [1]

B. High obstacle concentration ($F_o/F_g > 1$)

At high obstacle concentrations the flow "sees" no individual obstacles but a general terrain roughness.
This type of flow is also characterized as skimming flow because of the roller bearing action of the vortex flow between adjacent obstacles.

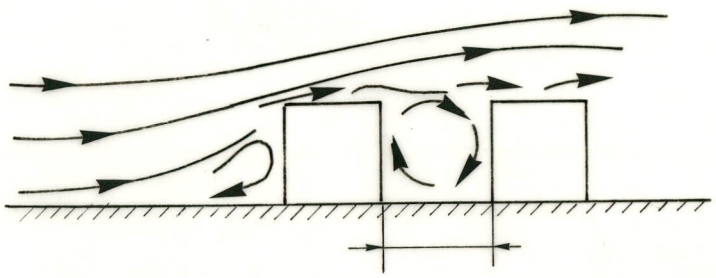

Figure 2.2 High obstacle concentration-schematized flow [1]

The flow downstream of the obstacle group may be considered as a rough wall boundary layer flow developing behind a rougness transition.
A method for calculation of the change in wind velocity downstream of a three-dimensional rougness transition is given a.o. by Vermeulen [2].

C. Intermediate obstacle concentration ($0.01 < F_o/F_g < 1.0$)

In the range of intermediate obstacle concentrations, when the obstacles are neither wide apart nor close together the obstacle formation is considered as a real group.
A method for estimating the effect on the local wind field is not available not even for simple group geometries.
A useful provisory approach to the problem is to categorize obstacle groups - depending on some features to be discussed below - as isolated obstacle or as a terrain rougness.

2.2 Obstacle fetch

The most important parameter for the flow developing from an obstacle group appears to be the group size, more specifically the dimension in the direction of the wind, called the fetch R.

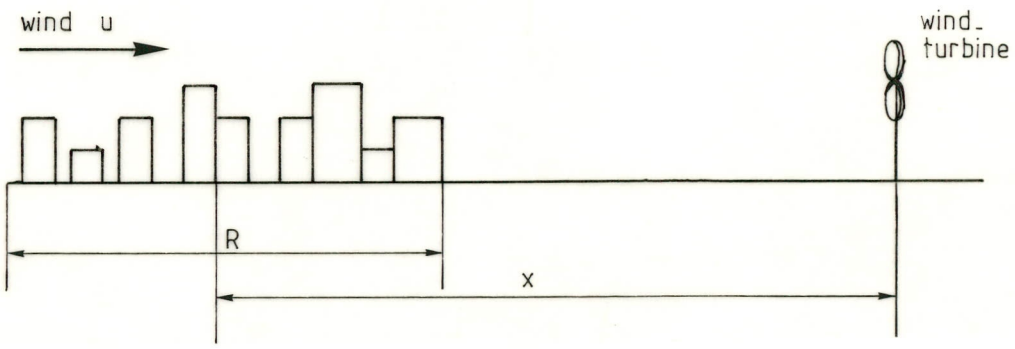

Figure 2.3 The fetch of an obstacle group

• small fetch

At small fetch the flow downsteam of the obstacle group shows a typical wake behaviour, similar to the situation of a single obstacle.
This means that both velocity- and turbulence profile vary with the distance x behind the obstacle group.
A reasonable approach is to consider the obstacle group as a wall with equal width as the group and a height equal to the mean obstacle height. In this way the standard wake effect graphs for single houses, or in case of small obstacle density the graph for (rows of) trees can be used.
This "substituting wall" concept has been applied earlier by [3] and appears to work well in case of the wind turbine site Camperduin [4], where a small residential quarter is present at a distance of x = 250 m.

• large fetch

At large fetch the flow downstream of the obstacle group shows a typical wall boundary layer character, similar to the flow over rough terrain.
Both the velocity and turbulence profile become irrespective of the distance x behind the obstacle group, i.e. the flow is in equilibrium.
The flow may be characterized with a roughness parameter z_o and the displacement height d in the well known logarithmic law of the wall. The calculation method for the wind velocity deficit at rotor height of a

wind turbine corresponds to that for a transition in terrain roughness, and is discussed in literature.
The effect of small groups with an enveloping angle - as seen from the wind turbine location - which is smaller than 15 deg. will be considered negligeable.
A complicating factor in determining the minimal fetch required for flow equilibrium, is its dependence on obstacle density λ_o.
By definition:

$$\lambda_o = F_o/O_g \qquad \text{if obstacle dimensions are known}$$

$$\text{or } \lambda_o = \frac{\bar{h}_{ob}}{\bar{d}_o} \cdot \frac{F_g}{O_g} \qquad \text{if only global obstacle information is available}$$

(F_o total frontal obstacle area; Og total terrain area; F_g area occupied by obstacles; $\bar{h}$ mean obstacle height; $\bar{d}$ mean obstacle depth)

An obstacle group can be categorized by means of figure A3.4, based on the work of Vermeulen [5] and Hussain [6].

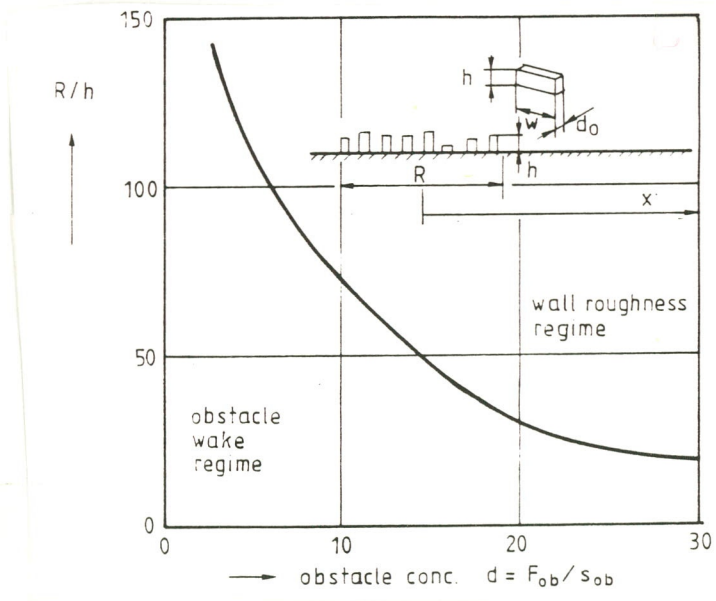

Figure 2.4 Fetch R required for the development of a stable wall boundary layer flow (best estimate from results of [5] and [6])

References

[1] Soliman, B.F.
"A study of the wind pressure forces acting on groups of buildings"
Univ. Sheffield, Oct. 1976.

[2] Vermeulen, P.E.J.
"Experiments on behalf of the model description of three-dimensional roughness changes"
MT-TNO rep. 86.201 (in Dutch), june 1986.

[3] Halitsky, J.
"Wake and dispersion models for the EBR-II building comples"
Atm. Env., Vol. 11, pp. 557-596, 1977.

[4] Leene, J.A.
"Obstacle wake effects and wind-turbine siting"
Delphi Workshop Wind En.Appl., 1985.

[5] Hussain, M.
"A study of the windforces on low rise buildings and their application to natural ventilation design methods"
Univ. of Sheffield, 1978.

[6] Vermeulen, P.E.J.
"Inventarisation and evaluation of methods to determine the local wind statistics"
MT-TNO, rep. 83-04376, april 1983.

Appendix A3 FLOW SPEED-UP OVER SIMPLE SHAPES

Obstacles in an atmospheric boundary layer not only cause the velocity decrease in the extensive wake zone but also induce a velocity increase in a much smaller area above and aside of the obstacle due to a deflection of the streamlines of the incoming wind flow by the obstacle and its wake.
In fact the velocity increase and decrease will be in balance as the total momentum is conserved.
The dimension of the zone with increased velocity depends, like the wake, on obstacle geometry.
An (almost) 2-dimensional obstacle like a mountain-ridge e.g. or at a smaller scale the edge of a wood or a dike will show the strongest effect. If the siting of a wind turbine in this so called speed-up zone is considered, because of the gain in available wind, it should be realized that the wind turbine must be small in relation to the relevant obstacle dimension (= the height when placing on top and the width when placing aside of the obstacle).
Beside, the wind turbine rotor should be able to withstand the fluctuating wind load caused by the velocity gradient along the rotor height or width.
For some simple obstacle shapes speed-up factors as given in literature will be presented hereafter.
In reality however the obstacle situation is often much more complicated and in those cases a wind tunnel study is recommended.

- Definitions

Several terms are used in literature to denote the velocity increase by an obstacle.
The velocity increase $\Delta u(z)$ at absolute height z (with respect to the same ground plane) in relation to the undisturbed wind velocity $U_o(z)$ is

$$\Delta u(z) = u(z) - u_o(z) \qquad (1)$$

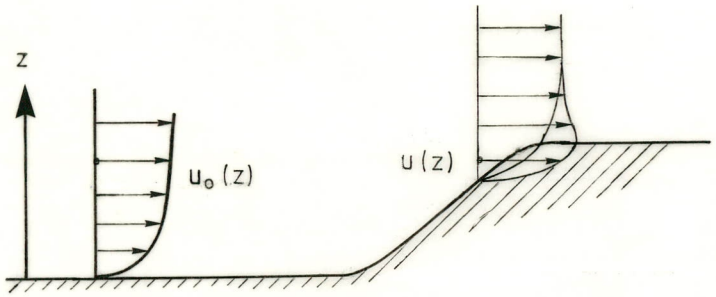

more often z is taken above local terrain as illustrated below.

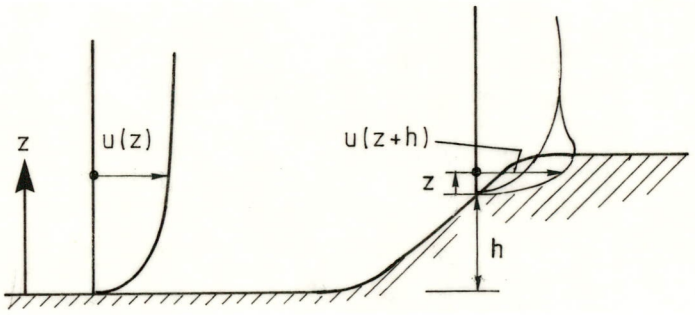

The fractional speed-up factor is defined then as

$$\Delta S = \frac{u\ (z+h) - u_o\ (z)}{u_o\ (z)} \qquad (2)$$

The relation between formula 1 and 2 is:

$$\Delta U = [(\Delta S + 1) - \frac{u_o\ (z+h)}{u_o\ (z)}\ ]\ u_o \qquad (3)$$

Another term sometimes used is the amplification factor G.

$$G = \frac{u\ (z+h)}{u_o\ (z)} \qquad (4)$$

$$\Delta S = G - 1 \qquad (5)$$

When velocities at equal absolute height - e.g. above sea level - are compared the term speed-up factor

is used $S = \frac{u\ (z+h)}{u_o\ (z+h)}$. (6)

The relation between ΔU and S is $\Delta U = (S-1).U_o\ (z+h)$
and between ΔS and S:

$$\Delta S = S.\frac{u_o(z+h)}{u_o\ (z)} - 1$$

• Formula for simple hill shapes

The approach of Lemelin et al [1] is used to describe the velocity increase for some simple obstacle shapes.
The term he uses to indicate the velocity increase is the fractional speed-up factor Δs. The in the context of the Handbook relevant part of his paper is cited below.

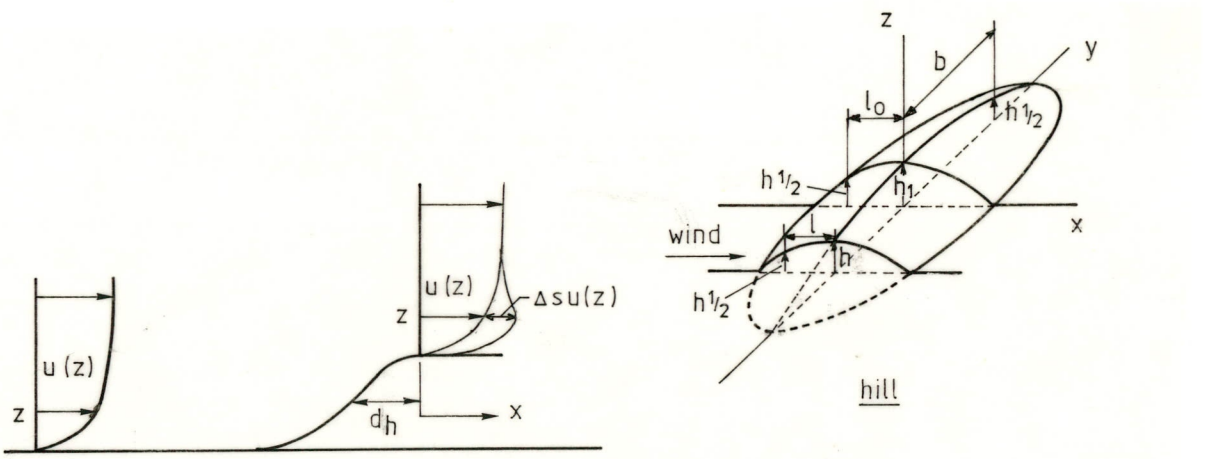

Figure 3.1 Definitions for wind speed-ups over hills

The formula used is:

$$\Delta S(x,z) = (\Delta S_{max})\ \left(\frac{1}{1 + 3(x/nd_h)^p}\right)^2 \left(\frac{1}{1 + a_s(z/d_h)}\right)^2 \qquad (7)$$

Where a_s, n and p are constants given in the next table.
The hill's length parameters in equation 7 are defined within a vertical plane containing the upstream wind vector and the point of interest on the hill (see figure 3.1); x represents the horizontal distance between the point of interest and the point of maximum height in that plane, h, where x = 0; and d_h is the characteristic halt-depth, equal to the hori-

zontal distance between x = 0 and the upstream point where the height in that plane is h/2. The hill height, h, is determined relative to a conservative average elevation of the terrain surrounding the hill and the variable height z is measured above local ground. Figure 3.2 presents the system of coordinates for 2Dimensional and 3Dimensional hill as well as escarpments. The values of "ΔS_{max}", "n" and "a" can be approximated by the following:

- 3Dimensional axisymmetric hills and 2Dimensional ridges (or valleys with h negative)

$$\Delta S_{max} = 2.3\ E\ \frac{w_h/d_{h_o}}{(w_h/d_{h_o} + 0.4)}$$

ø = h/L	E	d_{h_o}	a_s	n	p_s
≤ 0.4	ø	h/ø	2.0	2.0	2.0
> 0.4	0.4	2.5 h	2.0	2.0	2.0

The aspect ratio, w_h/d_h, is a representation of the overall shape of the hill for the given wind direction. The parameter w_h is the half-width i.e. the distance between the highest point on the hill and half that value in the across-wind direction and d_{h_o} is the distance between the highest point and half that value, upstream in the along-wind direction. For an asymmetric hill, the parameter w_h should be taken from the side which gives the largest distance. In the particular case where the plane of interest passes through the point of highest elevation, then $d_h = d_{h_o}$ and h is the maximum height of the hill.

- 2dimensional escarpments

$\Delta S_{max} = 1.3\ E$

$\phi = h/d_h$ max	E	$d_h$max	a_s		n	p_s
≤ 1.0	ϕ	h/ϕ	2.0	x ≤ 0	1.0	2.0
				x > 0	5.0	1.0
> 1.0	1.0	h	0.6	x ≤ 0	0.5	2.0
				x > 0	10.0	1.0

- Embankments

Speed-ups over embankments can be treated like escarpments when the horizontal downstream plateau is greater than $2d_h$. When the plateau is smaller than $2d_h$,the embankment should be regarded as a ridge.

An illustration of the accuracy of the Lemelin approach is given in figures A3.3 and A3.4 where a comparison with results of other research work has been made.

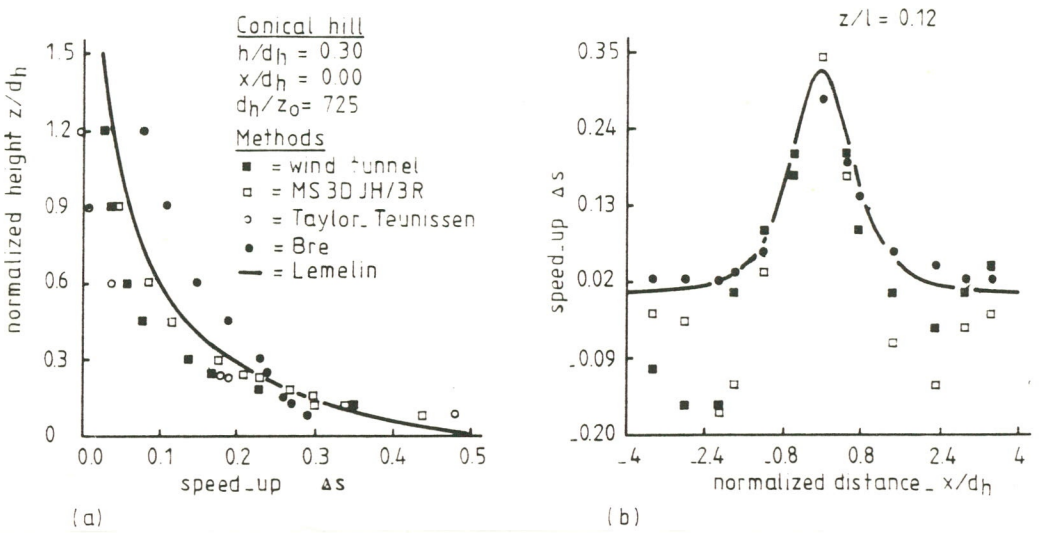

Figure 3.2 Speed-up profiles above a conical hill

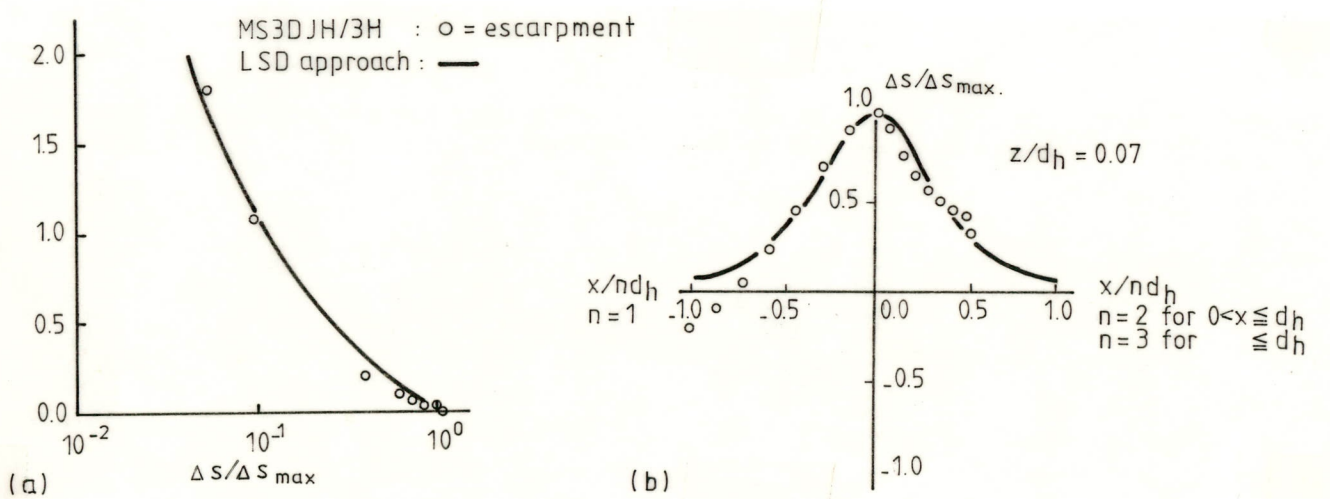

(a) (b)

Figure 3.3 Variation of $\Delta S/\Delta S_{max}$ (a) with height on the brow of escarpments and (b) with distance from the brow of escarpments

The figures show a wide scatter of datapoints and reasonable good agreement with possibly some overestimation of speed-up with horizontal distance from the crest.

The figures also clearly illustrate the relatively small extent of the speed-up zone. For the conical hill at $z/_1 = 1$ the speed-up has already dropped from a value as high as 50% at $z/_1 = 0$ to a value of some 5%. For the escarpment the equivalent values are 100% at $z/_1 = 0$ to 10% at $z/_1 = 1$. It also underlines the steepness of the local wind gradient.
So with regard to siting wind turbines on hills, dikes or other terrain elevations speed-up appears to be of importance only in those cases where the hill dimensions - characteristic length L - are large in relation to the wind turbine axis height.
It should also be realized that part of the speed-up as given in formulae 6 and 7 and is only an effect of the height increase of the wind turbine axis in the wind gradient.
From $u_2 = u * \frac{1}{\kappa} \ln z/z_o$
it can be deduced that

$$\Delta S = \frac{\ln z_2/z_1}{\ln z_1/z_o}$$

Some calculated values of ΔS for an arbitrary situation of terrain roughness $z_o = 0.03$ m axis height $z_1 = 25$ m are given below.

z_2 [m]	ΔS [%]
25	0
35	5
45	8.7
55	11.7

The flow passing a hill also undergoes an effect on turbulence.
From [2] it appears that over the height relevant to wind turbine rotors the longitudinal component of turbulence decreases appreciably.
For 2-dimensional hills the relative change of the turbulence variance at $x/_L = 0$ (the crest) with respect to its undisturbed value is:

$$\frac{\Delta\sigma_u^2}{\sigma_u^2} = -\frac{4}{5}\Delta S$$

Summarizing, locating a wind turbine very close to a hill or other terrain elevation, generally gives a velocity increase and turbulence decrease, but possibly a stronger wind shear along the rotor blade.
The effect is only important for terrain elevations which are large compared to the wind turbine hub height.

References

[1] Lemelin, D.R., Surry, D. et al.
"Simple approximations for wind speed-up over hills".
J. Wind Engineering, Vol. 28, pp. 117-127, 1988.

[2] Hoff, A.M., Tetzlaff, H.
"Experimental investigations of the air flow over a nearly two-dimensional hill".
Meteor. Rundschau, Vol. 39, pp. 113-126, aug. 1986.